

Heavy-flavor production in global QCD analyses

Marco Guzzi

Kennesaw State University

with

A. Ablat, S. Dulat, T.-J. Hou, P. Nadolsky

I. Sitiwaldi, K. Xie, and C.-P. Yuan



KENNESAW STATE
UNIVERSITY



QCD@Work 2022 International Workshop on QCD: Theory and Experiment.
Lecce, IT, June 27-30, 2022 (June 28, 2022)



This talk

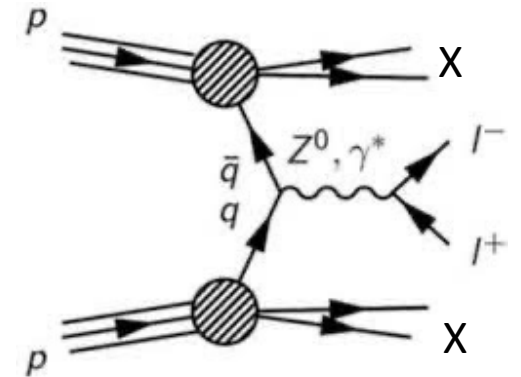
- Impact of Heavy-Flavor (HF) production at hadron colliders on the structure of the proton:
c/b production @LHCb13, $t\bar{t}$ @LHC13, c/b production @HERA
- HF treatments in precision theory predictions
- Results of recent studies **beyond** the latest global QCD analysis from the CTEQ-TEA group (CT18 PDFs Phys. Rev. D (2021))

A long story short: Parton Distribution Functions (PDFs) of the proton are essential ingredients of factorization theorems in QCD.

e.g., for Drell-Yan we have (Collins Soper Serman (1984), (1985))

$$\sigma(h_1 h_2 \rightarrow l^+ l^- + X) = \sum_{a,b} \int_{x_1}^1 d\xi_1 \int_{x_2}^1 d\xi_2 f_{h_1 \rightarrow a}(\xi_1, \alpha_s(\mu_R), \mu_R, \mu_F) f_{h_2 \rightarrow b}(\xi_2, \alpha_s(\mu_R), \mu_R, \mu_F) \times \hat{\sigma}^{ab}\left(\frac{x_1}{\xi_1}, \frac{x_2}{\xi_2}; \alpha_s(\mu_R), Q, \mu_F, \mu_R\right) + \mathcal{O}\left(\frac{\Lambda^2}{Q^2}\right), \quad (1)$$

long-distance non-perturbative contributions (PDFs)



short-distance infrared-safe perturbatively calculable quantities (hard scatterings)

Differently from hard-scatterings, the analytic structure of the PDFs cannot be predicted by perturbative QCD but must be determined by comparing standard sets of cross sections, such as Eq. 1, to experimental measurements by using a variety of analytical methods.

For this reason, PDFs are “data-driven” quantities.

Important input for TMDs

Motivations I (what are data telling us?)

Goals:

- Assess the impact of heavy-flavor (HF) production on unpolarized PDFs
- Improve PDF uncertainties in global QCD analyses (in particular, constrain HF PDFs)
- Probe QCD dynamics at small and large x (x = longitudinal momentum fraction of struck parton in the proton).

Important for: precision BSM searches, precise and accurate theory predictions (pQCD),...

Heavy-flavor treatment in theory predictions (GMVFN schemes):

- DIS: S-ACOT- χ (default in CTEQ analyses) based on Collins' HF factorization in DIS
- Extend the S-ACOT GMVFN scheme to PP collisions: S-ACOT-MPS. Now at NLO. NNLO needed.
- Implemented for inclusive charm [[FPF, 2109.10905, 2203.05090](#)] and bottom [[2203.06207](#)] production.
- S-ACOT-MPS can be extended to other processes.

Motivations II

- Heavy-quark production at the LHC at small p_T and large rapidity y of the heavy quark: sensitive to PDFs at both small and large x (especially true for c/b production)

$$x_{1,2} \approx \frac{\sqrt{p_T^2 + m_Q^2}}{\sqrt{S}} e^{\pm y}$$

- In this kinematic region PDFs are poorly constrained by other experiments in global PDF fits.
- In particular, c/b production in the $4 < |y| < 4.5$ rapidity range in pp collisions at the LHC 13 TeV can probe $x \leq 10^{-5}$. When $p_T \geq 40$ GeV, it can probe $x \geq 0.2$
- Top-quark pair production @LHC can probe the gluon PDF already at $x \gtrsim 0.01$
- c/b prod. @HERA sensitive to intermediate and small x

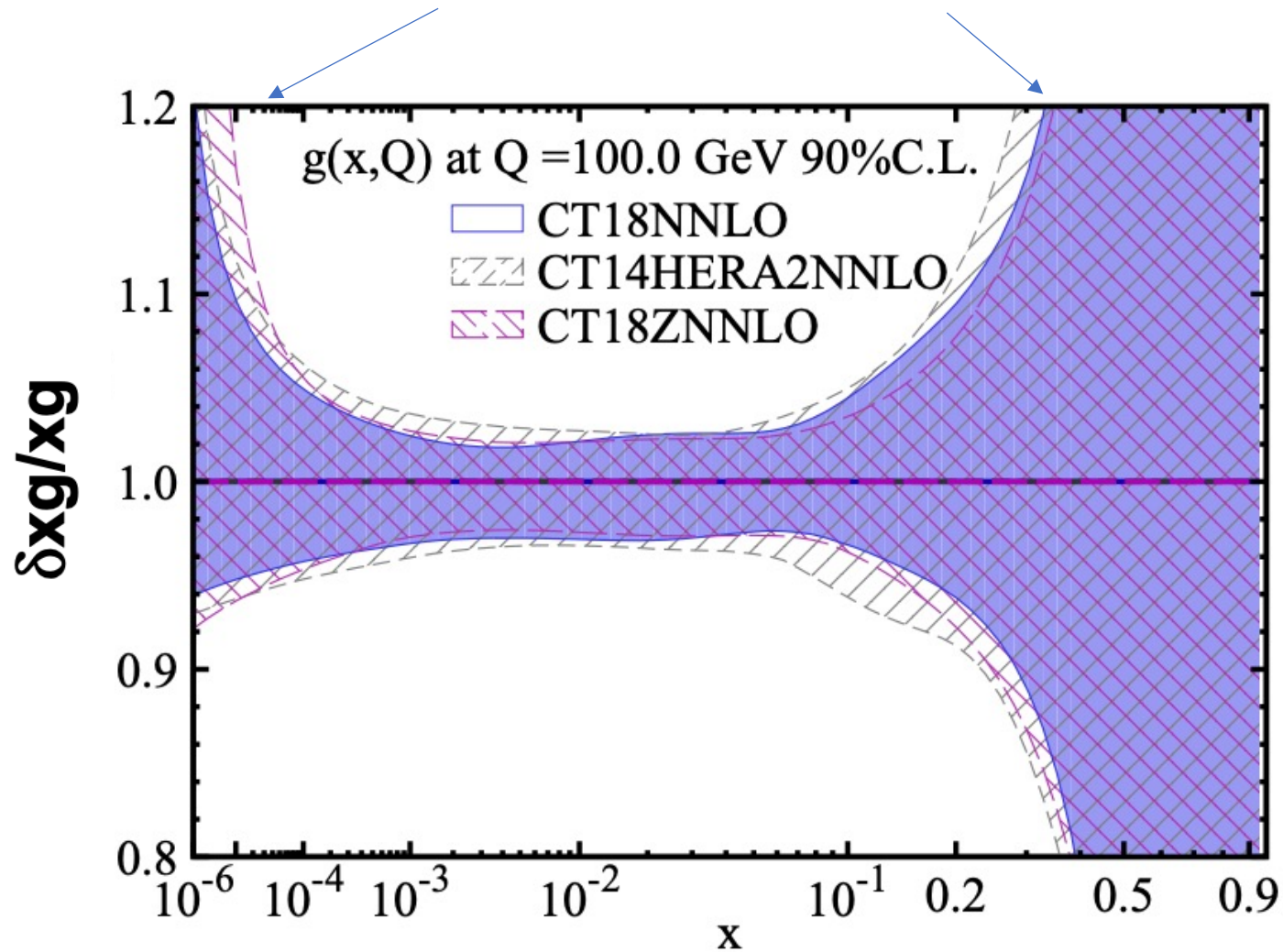


Figure: CT18 gluon PDF, *Phys. Rev. D* 103 (2021). Small- and large- x regions have wide uncertainty bands. See also: The PDF4LHC21 combination of global PDF fits for the LHC Run III, 2203.05506 [hep-ph] (More about it in E. Nocera's talk on Wed.)

Motivations II

- Probing this regime (and beyond, at future facilities) helps us shed light on interesting problems: **(intrinsic) heavy-flavor content** of the proton, and on **small-x dynamics**.
- LHC delivered precise measurements for these observables, (e.g., $t\bar{t}$ prod. at **ATLAS** and **CMS**; D-meson prod. at **LHCb**).
- In addition, we have the **HERA** legacy: most recent c/b production combination in DIS

The CT18 analysis

New CTEQ global analysis of quantum chromodynamics with high-precision data from the LHC

Tie-Jiun Hou,^{1,†} Jun Gao,² T. J. Hobbs,^{3,4} Keping Xie,^{3,5} Sayipjamal Dulat,^{6,‡} Marco Guzzi,⁷ Joey Huston,⁸ Pavel Nadolsky,^{3,8} Jon Pumplin,^{8,*} Carl Schmidt,⁸ Ibrahim Sitiwaldi,⁶ Daniel Stump,⁸ and C.-P. Yuan^{8,||}

TABLE I. Datasets included in the CT18(Z) NNLO global analyses. Here we directly compare the quality of fit found for CT18 NNLO vs CT18Z NNLO on the basis of χ^2_E , $\chi^2_E/N_{pt,E}$, and S_E , in which $N_{pt,E}$, χ^2_E are the number of points and value of χ^2 for experiment E at the global minimum. S_E is the effective Gaussian parameter [38,42,56] quantifying agreement with each experiment. The ATLAS 7 TeV 35 pb⁻¹ W/Z dataset, marked by ‡, is replaced by the updated one (4.6 fb⁻¹) in the CT18A and CT18Z fits. The CDHSW data, labeled by †, are not included in the CT18Z fit. The numbers in parentheses are for the CT18Z NNLO fit.

Exp. ID#	Experimental dataset	$N_{pt,E}$	χ^2_E	$\chi^2_E/N_{pt,E}$	S_E
160	HERAI + II 1 fb ⁻¹ , H1 and ZEUS NC and CC $e^\pm p$ reduced cross sec. comb.	[30]	1120	1408 (1378)	1.3 (1.2) 5.7 (5.1)
101	BCDMS F_2^p	[57]	337	374 (384)	1.1 (1.1) 1.4 (1.8)
102	BCDMS F_2^d	[58]	250	280 (287)	1.1 (1.1) 1.3 (1.6)
104	NMC F_2^d/F_2^p	[59]	123	126 (116)	1.0 (0.9) 0.2 (-0.4)
108 [†]	CDHSW F_2^p	[60]	85	85.6 (86.8)	1.0 (1.0) 0.1 (0.2)
109 [†]	CDHSW $x_B F_3^p$	[60]	96	86.5 (85.6)	0.9 (0.9) -0.7 (-0.7)
110	CCFR F_2^p	[61]	69	78.8 (76.0)	1.1 (1.1) 0.9 (0.6)
111	CCFR $x_B F_3^p$	[62]	86	33.8 (31.4)	0.4 (0.4) -5.2 (-5.6)
124	NuTeV $\nu\mu\mu$ SIDIS	[63]	38	18.5 (30.3)	0.5 (0.8) -2.7 (-0.9)
125	NuTeV $\bar{\nu}\mu\mu$ SIDIS	[63]	33	38.5 (56.7)	1.2 (1.7) 0.7 (2.5)
126	CCFR $\nu\mu\mu$ SIDIS	[64]	40	29.9 (35.0)	0.7 (0.9) -1.1 (-0.5)
127	CCFR $\bar{\nu}\mu\mu$ SIDIS	[64]	38	19.8 (18.7)	0.5 (0.5) -2.5 (-2.7)
145	H1 σ_p^c	[65]	10	6.8 (7.0)	0.7 (0.7) -0.6 (-0.6)
147	Combined HERA charm production	[66]	47	58.3 (56.4)	1.2 (1.2) 1.1 (1.0)
169	H1 F_L	[33]	9	17.0 (15.4)	1.9 (1.7) 1.7 (1.4)
201	E605 Drell-Yan process	[67]	119	103.4 (102.4)	0.9 (0.9) -1.0 (-1.1)
203	E866 Drell-Yan process $\sigma_{pd}/(2\sigma_{pp})$	[68]	15	16.1 (17.9)	1.1 (1.2) 0.3 (0.6)
204	E866 Drell-Yan process $Q^3 d^2\sigma_{pp}/(dQ dx_F)$	[69]	184	244 (240)	1.3 (1.3) 2.9 (2.7)
225	CDF run-1 lepton A_{ch} , $p_{T\ell} > 25$ GeV	[70]	11	9.0 (9.3)	0.8 (0.8) -0.3 (-0.2)
227	CDF run-2 electron A_{ch} , $p_{T\ell} > 25$ GeV	[71]	11	13.5 (13.4)	1.2 (1.2) 0.6 (0.6)
234	DØ run-2 muon A_{ch} , $p_{T\ell} > 20$ GeV	[72]	9	9.1 (9.0)	1.0 (1.0) 0.2 (0.1)
260	DØ run-2 Z rapidity	[73]	28	16.9 (18.7)	0.6 (0.7) -1.7 (-1.3)
261	CDF run-2 Z rapidity	[74]	29	48.7 (61.1)	1.7 (2.1) 2.2 (3.3)
266	CMS 7 TeV 4.7 fb ⁻¹ , muon A_{ch} , $p_{T\ell} > 35$ GeV	[75]	11	7.9 (12.2)	0.7 (1.1) -0.6 (0.4)
267	CMS 7 TeV 840 pb ⁻¹ , electron A_{ch} , $p_{T\ell} > 35$ GeV	[76]	11	4.6 (5.5)	0.4 (0.5) -1.6 (-1.3)
268 [‡]	ATLAS 7 TeV 35 pb ⁻¹ W/Z cross sec., A_{ch}	[77]	41	44.4 (50.6)	1.1 (1.2) 0.4 (1.1)
281	DØ run-2 9.7 fb ⁻¹ electron A_{ch} , $p_{T\ell} > 25$ GeV	[78]	13	22.8 (20.5)	1.8 (1.6) 1.7 (1.4)
504	CDF run-2 inclusive jet production	[79]	72	122 (117)	1.7 (1.6) 3.5 (3.2)
514	DØ run-2 inclusive jet production	[80]	110	113.8 (115.2)	1.0 (1.0) 0.3 (0.4)

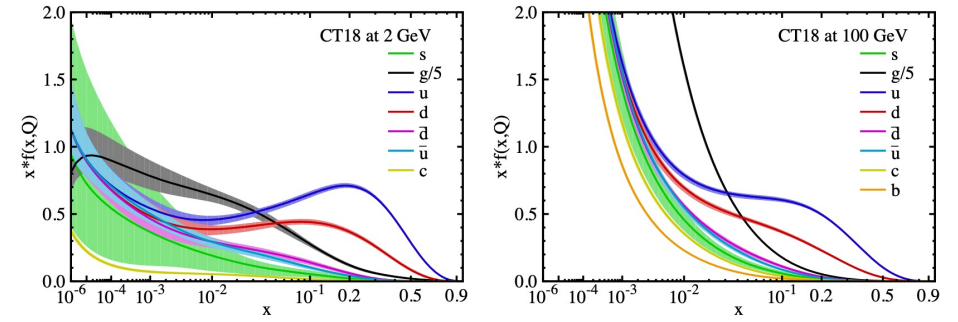


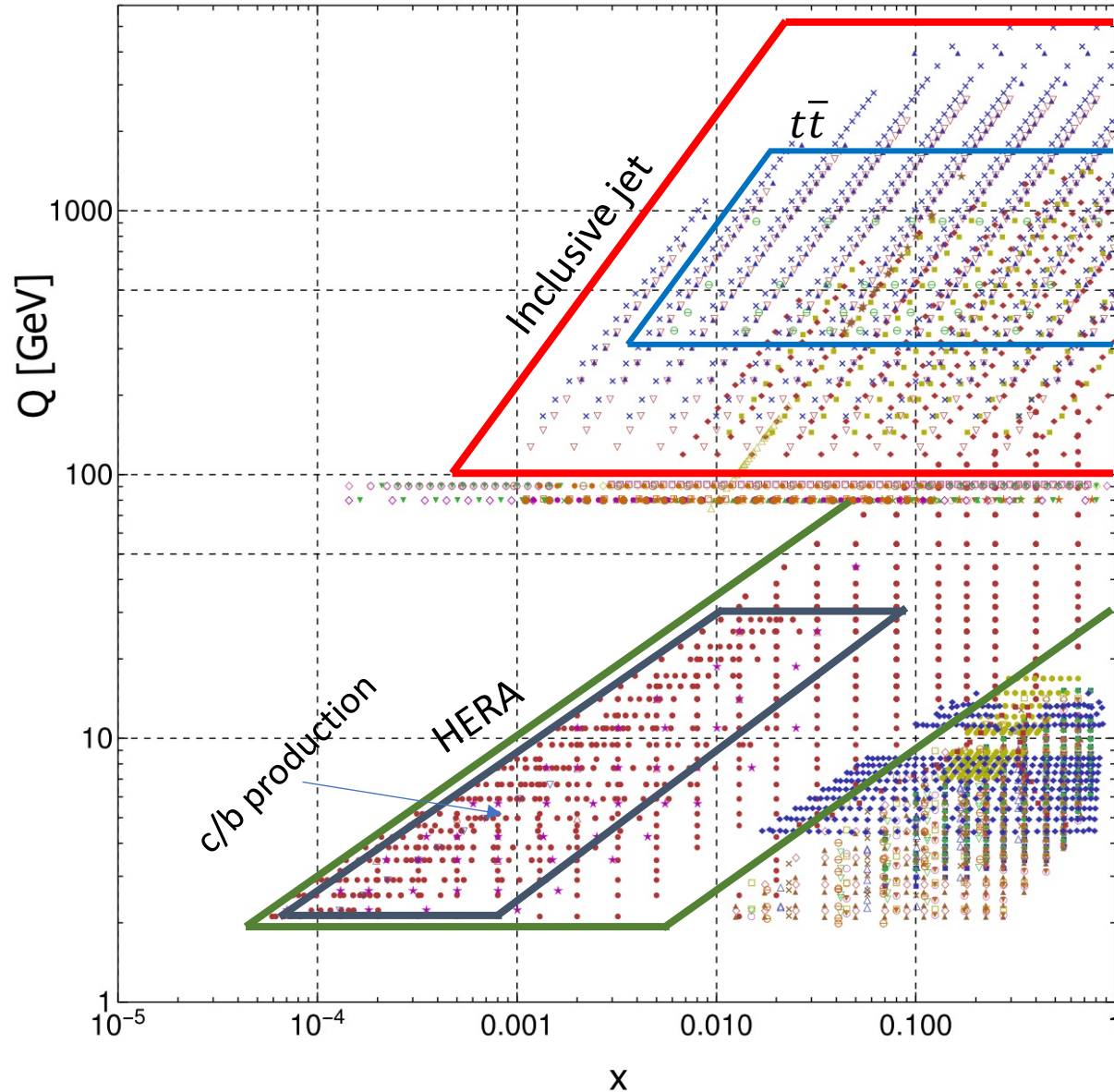
TABLE II. Like Table I, for newly included LHC measurements. The ATLAS 7 TeV W/Z data (4.6 fb⁻¹), labeled by ‡, are included in the CT18A and CT18Z global fits, but not in CT18 and CT18X.

Exp. ID#	Experimental dataset	$N_{pt,E}$	χ^2_E	$\chi^2_E/N_{pt,E}$	S_E
245	LHCb 7 TeV 1.0 fb ⁻¹ W/Z forward rapidity cross sec.	[81]	33	53.8 (39.9)	1.6 (1.2) 2.2 (0.9)
246	LHCb 8 TeV 2.0 fb ⁻¹ $Z \rightarrow e^-e^+$ forward rapidity cross sec.	[82]	17	17.7 (18.0)	1.0 (1.1) 0.2 (0.3)
248 [‡]	ATLAS 7 TeV 4.6 fb ⁻¹ , W/Z combined cross sec.	[39]	34	287.3 (88.7)	8.4 (2.6) 13.7 (4.8)
249	CMS 8 TeV 18.8 fb ⁻¹ muon charge asymmetry A_{ch}	[83]	11	11.4 (12.1)	1.0 (1.1) 0.2 (0.4)
250	LHCb 8 TeV 2.0 fb ⁻¹ W/Z cross sec.	[84]	34	73.7 (59.4)	2.1 (1.7) 3.7 (2.6)
253	ATLAS 8 TeV 20.3 fb ⁻¹ , $Z p_T$ cross sec.	[85]	27	30.2 (28.3)	1.1 (1.0) 0.5 (0.3)
542	CMS 7 TeV 5 fb ⁻¹ , single incl. jet cross sec., $R = 0.7$ (extended in y)	[86]	158	194.7 (188.6)	1.2 (1.2) 2.0 (1.7)
544	ATLAS 7 TeV 4.5 fb ⁻¹ , single incl. jet cross sec., $R = 0.6$	[9]	140	202.7 (203.0)	1.4 (1.5) 3.3 (3.4)
545	CMS 8 TeV 19.7 fb ⁻¹ , single incl. jet cross sec., $R = 0.7$ (extended in y)	[87]	185	210.3 (207.6)	1.1 (1.1) 1.3 (1.2)
573	CMS 8 TeV 19.7 fb ⁻¹ , $t\bar{t}$ norm. double-diff. top p_T and y cross sec.	[88]	16	18.9 (19.1)	1.2 (1.2) 0.6 (0.6)
580	ATLAS 8 TeV 20.3 fb ⁻¹ , $t\bar{t}$ p_T^t and $m_{t\bar{t}}$ abs. spectrum	[89]	15	9.4 (10.7)	0.6 (0.7) -1.1 (-0.8)

Heavy-flavor production measurements at HERA and LHC included in the CT18 NNLO QCD global analysis.

PDF Kinematics: the Q - x plane

Experimental data in CT18 PDF analysis



● HERAI+II'15	◇ ZyCDF2'10
■ BCDMSp'89	△ HERAB'06
◆ BCDMSb'90	▽ HERA-FL'11
▲ NMCrat97	× CMS7EASY'12
▼ CDHSW-F2'91	⊙ ATL7WZ'12
○ CDHSW-F3'91	★ D02EASY2'15
□ CCFR-F2'01	● CMS7MASY2'14
◇ CCFR-F3'97	■ CDF2JETS'09
△ NuTeV-NU'06	◆ D02JETS'08
▽ NuTeV-NUB'06	▲ ATLAS7JETS'15
× CCFR SI NU'01	▼ LHCb7ZWRAP'15
⊙ CCFR SI NUB'01	○ LHCb8ZEE'15
★ HERAc'13	□ CMS8WASY'16
● E605'91	◇ LHCb8WZ'16
■ E866RAT'01	△ ATL8ZPT'16
◆ E866PP'03	▽ CMS7JETS'14
▲ CDF1WASY'96	× CMS8JETS'17
▼ CDF2WASY'05	⊙ CMS8TTB-PTTYT'17
○ D02MASY'08	★ ATL8TTB-PTT-MTT'15
□ ZyD02'08	● ATL7ZW'16

Jet and $t\bar{t}$ complement each other in the kinematic plane. They impact the **gluon PDF at large x** . Important to disentangle the effect due to jet production and top-quark data.

Top and jet Data in CT18

- Top-quark
- 1511.04716 ATLAS 8 TeV $t\bar{t}$ ptT diff. distributions
 - 1511.04716 ATLAS 8 TeV $t\bar{t}$ mTT diff. distributions
 - 1703.01630 CMS 8 TeV $t\bar{t}$ (p_T, y_T) 2d diff. distrib.
- Jet production
- 1406.0324 CMS incl. jet at 7 TeV with $R=0.7$
 - 1410.8857 ATLAS incl. jet at 7 TeV with $R=0.6$
 - 1609.05331 CMS incl. jet at 8 TeV with $R=0.7$

CT18 includes two $t\bar{t}$ 1D differential observables from ATLAS (using statistical correlations) and double differential measurements from CMS in order to include as much information as possible. Some of the observables are in tension with each other.

HF treatments in theory calculations

Heavy-flavor production dynamics is nontrivial due to the interplay of massless and massive schemes which are different ways of organizing the perturbation series

Massive Schemes: final-state HQ with $p_T \leq m_Q \Rightarrow p_T$ -spectrum can be obtained in the **fixed-flavor number (FFN) scheme**.

- No heavy-quark PDF in the proton. Heavy flavors generated as massive final states. m_Q is an infrared cut-off.
- Power terms $(p_T^2/m_Q^2)^p$ are correctly accounted for in the perturbative series.

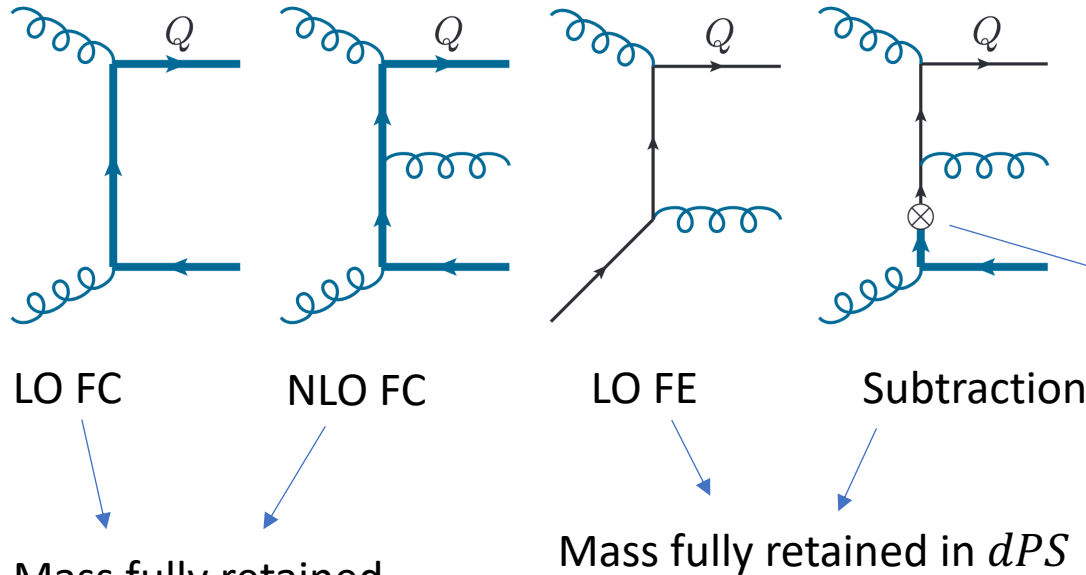
Massless schemes: $p_T \gg m_Q \gg m_P \Rightarrow$ appearance of log terms $\alpha_s^m \log^n (p_T^2/m_Q^2)$ that spoil the convergence of the fixed-order expansion. Essentially, a **zero mass (ZM) scheme**.

- Heavy quark is considered essentially massless and enters also the running of α_s .
- Need to resum these logs with DGLAP: initial-state logs resummed into a heavy-quark PDF, final-state logs resummed into a fragmentation function (FF)

Interpolating (GMVFN) schemes: composite schemes that retain key mass dependence and efficiently resum collinear logs, so that they combine FFN and ZM schemes together. They are crucial for:

- a correct treatment of heavy flavors in DIS and PP,
- accurate predictions of key scattering rates at the LHC,
- global analyses to determine proton PDFs.

Main idea behind a GMVNS (S-ACOT-MPS)



The subtraction term avoids double counting and cancels enhanced collinear contributions from FC when $\hat{s} \gg m_Q^2$ or $p_T \gg m_Q$

Collinear splitting $gg \rightarrow Q\bar{Q}$

Mass fully retained in $\hat{\sigma}$ and dPS

Mass fully retained in dPS

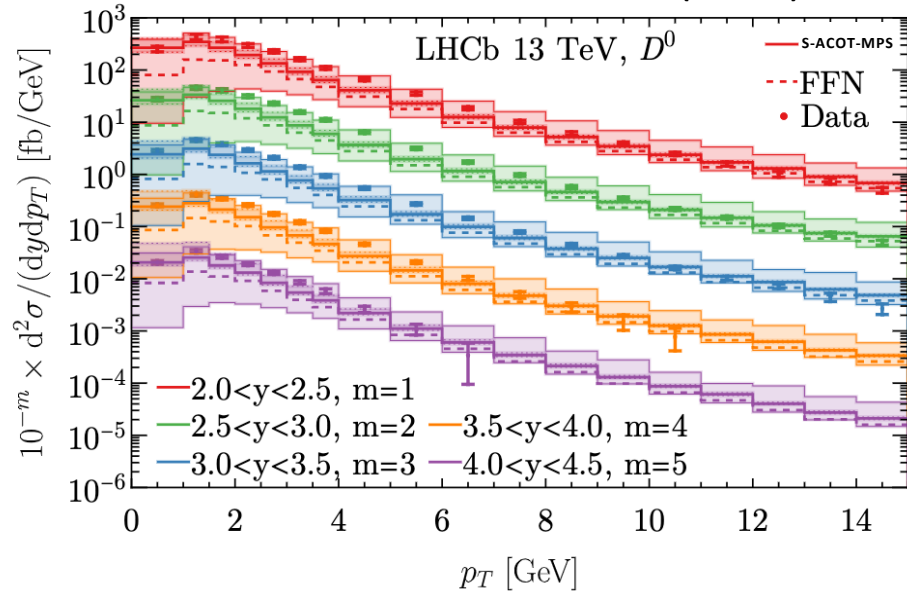
allows us to get (FE-Subtraction) in one step

$$\sigma = \text{FC} + \text{FE} - \text{SB.} \quad \text{Subtraction well defined also in the } p_T \rightarrow 0 \text{ limit}$$

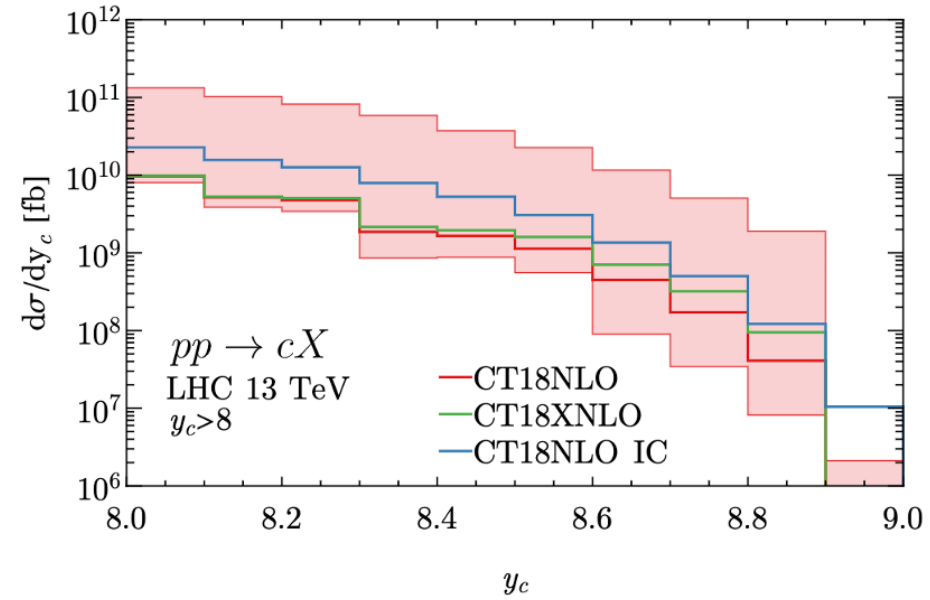
FE and Subtraction \rightarrow facilitated by introducing residual PDF: $\delta f_Q(x, \mu^2) = f_Q(x, \mu^2) - \frac{\alpha_s}{2\pi} \log\left(\frac{\mu^2}{m_Q^2}\right) f_Q(x, \mu^2) \otimes P_{Q \leftarrow g}(x)$

Charm production at central and forward rapidity

LHCb 13 TeV data: JHEP 03 (2016) 159

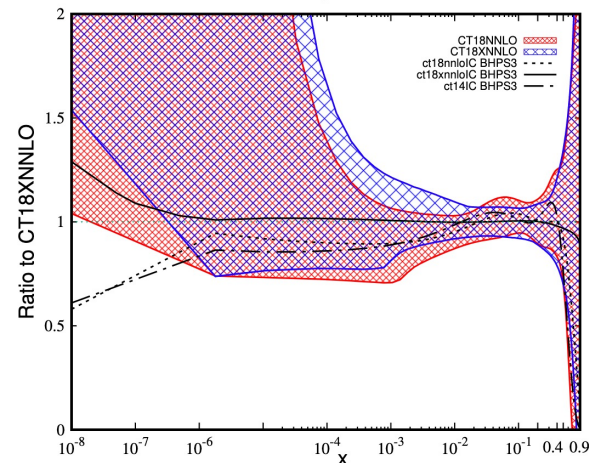


Transverse momentum at central rapidity at LHCb 13TeV. Error bands are scale uncertainties. [\[arXiv:2108.03741\]](https://arxiv.org/abs/2108.03741)



Rapidity distributions of prompt charm at the LHC 13 TeV in the very forward region ($y_c > 8$). Error band represents the CT18NLO induced PDF uncertainty at 68% C.L. [\[arXiv:2109.10905\]](https://arxiv.org/abs/2109.10905)

Gluon PDF, $Q = 2 \text{ GeV}$



NNLO gluon PDF in CT18/CT18X with Intrinsic Charm. Error PDFs at 90% C.L. [\[Phys. Rep. 968 \(2022\) 2109.10905\]](https://arxiv.org/abs/2109.10905)

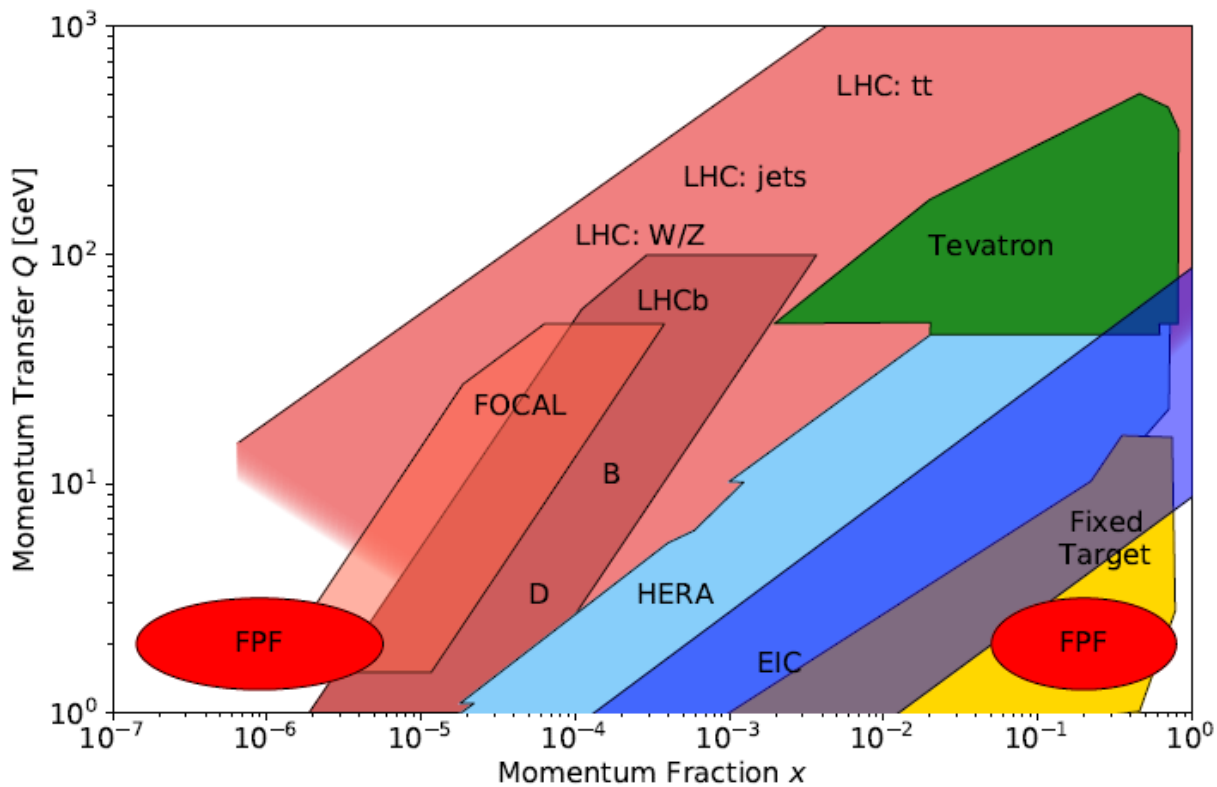
Charm hadroproduction and $Z + c$ production at the LHC can constrain the IC contributions. In CT14IC, we looked at $Z+c$ at LHC 8 and 13 TeV. LHCb $Z+c$ data deserve attention as they can potentially discriminate gluon functional forms at $x \geq 0.2$ and improve gluon accuracy.

For small x below 10^{-4} , higher-order QCD terms with $\ln(1/x)$ dependence grow quickly at factorization scales of order 1 GeV. FPF facilities like FASERv will access a novel kinematic regime where both large- x and small- x QCD effects contribute to charm hadroproduction rate.

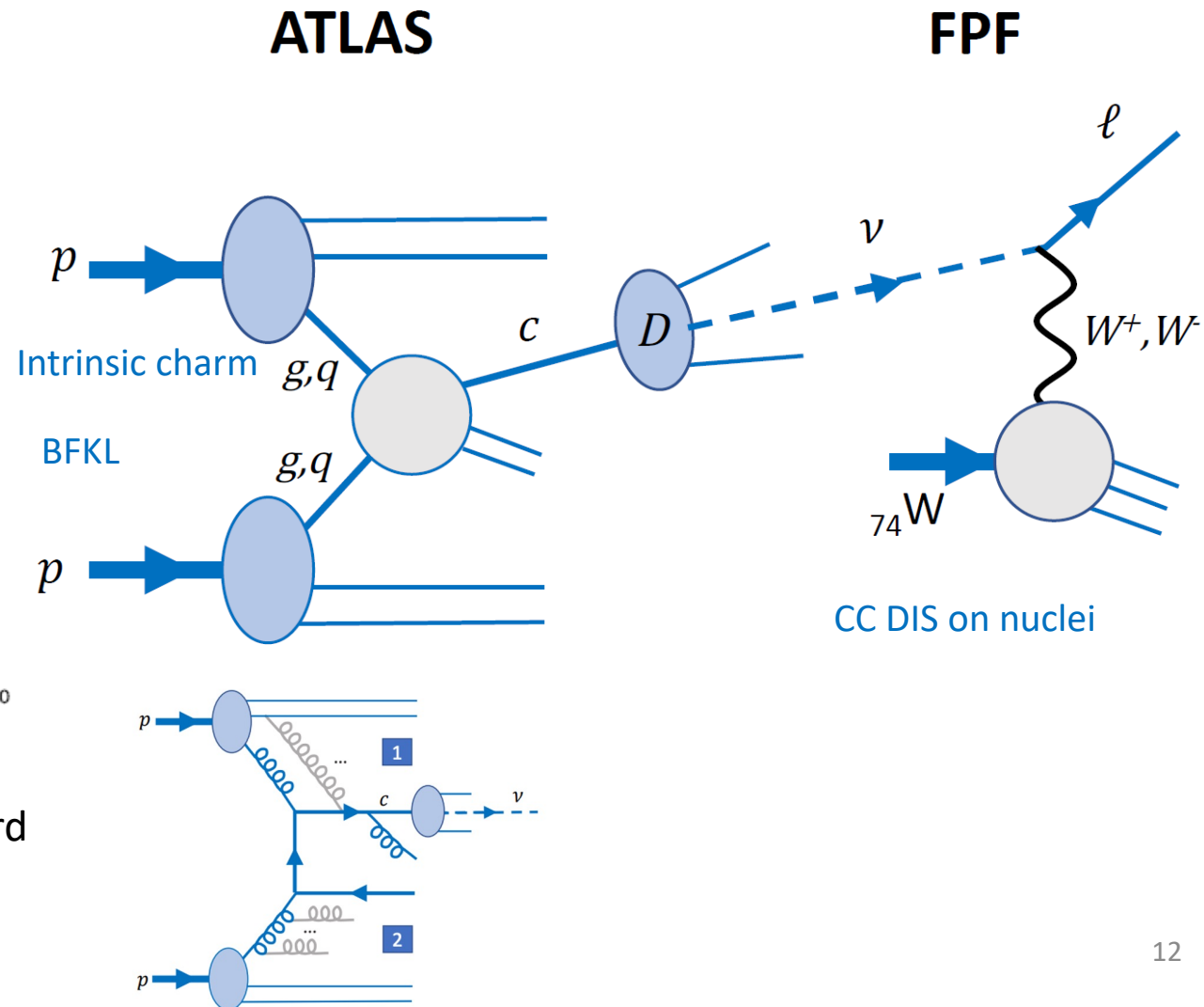
The Forward Physics Facility at CERN

L.A. Anchordoqui et al., "The Forward Physics Facility: Sites, Experiments, and Physics Potential", *Phys. Rep.* 968 (2022), [arXiv:2109.10905](https://arxiv.org/abs/2109.10905)

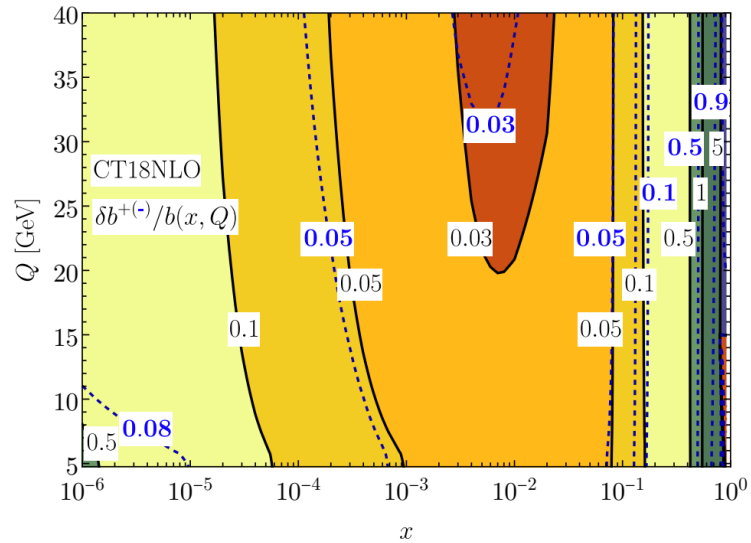
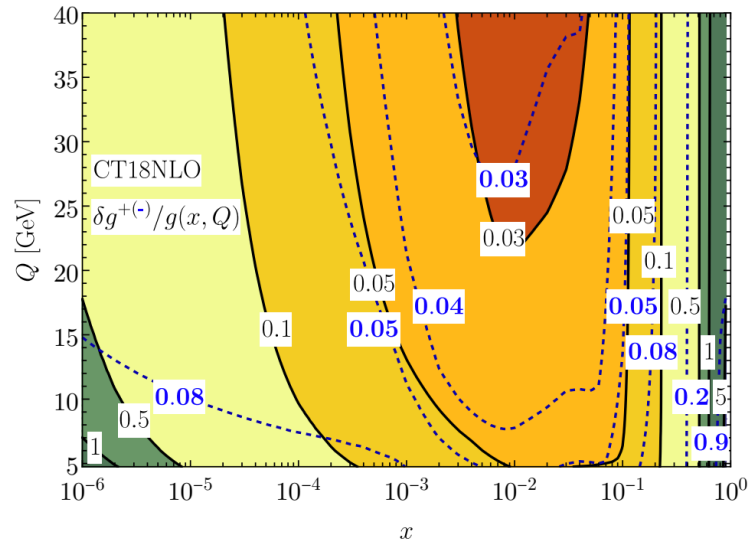
J.L. Feng et al., "The Forward Physics Facility at the High-Luminosity LHC", [arXiv:2203.05090](https://arxiv.org/abs/2203.05090)



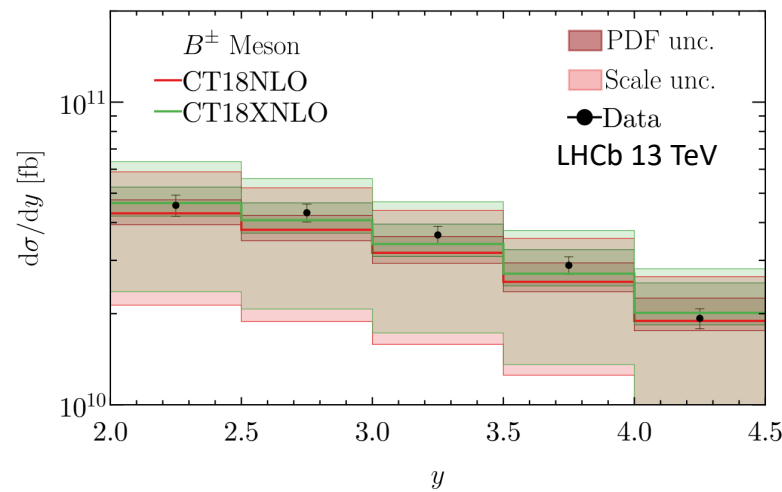
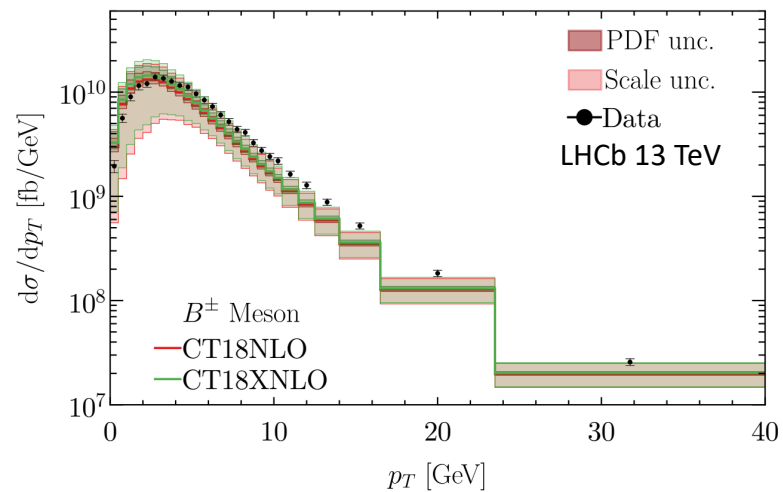
The FPF can clarify multiple aspects of QCD in the new forward region **in coordination** with the HL-LHC and EIC.



Inclusive b-production



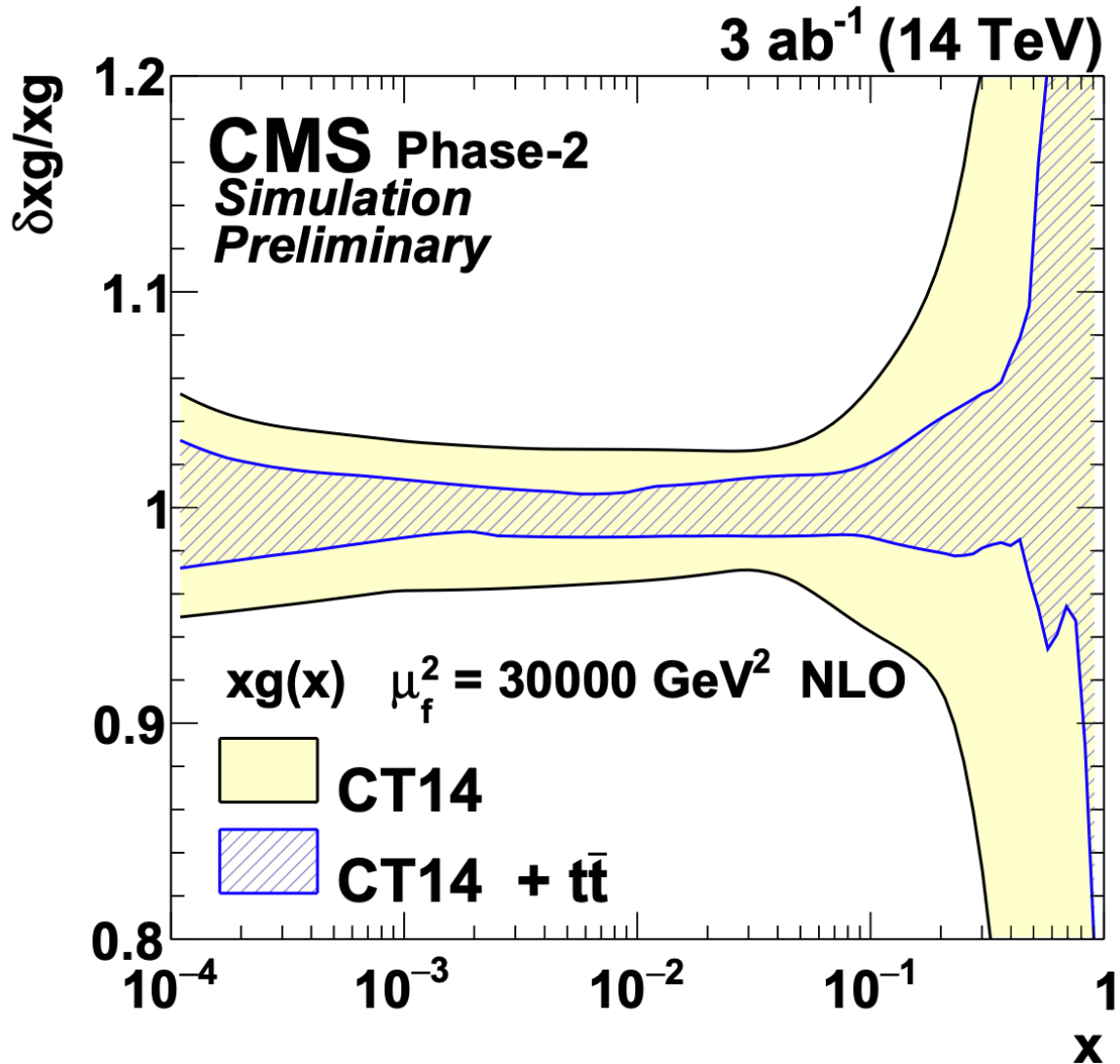
Strong sensitivity to the gluon and the b-quark PDFs. Corresponding PDF uncertainties obtained with the asymmetric Hessian approach at the 90% CL, with positive (negative) direction denoted as black solid (blue dashed) lines
[\[Xie, M.G., Nadolsky, 2203.06207\]](#)



NLO theory predictions for the p_T and y distributions obtained with CT18NLO and CT18XNLO PDFs compared to B^\pm production data from LHCb 13 TeV
[\[Xie, M.G., Nadolsky, 2203.06207\]](#)

Theoretical uncertainties at NLO are large ($O(50\%)$) and mainly ascribed to scale variation. This can be improved by including higher-order corrections which imply an extension of the S-ACOT-MPS scheme to NNLO

How constraining are $t\bar{t}$ data?



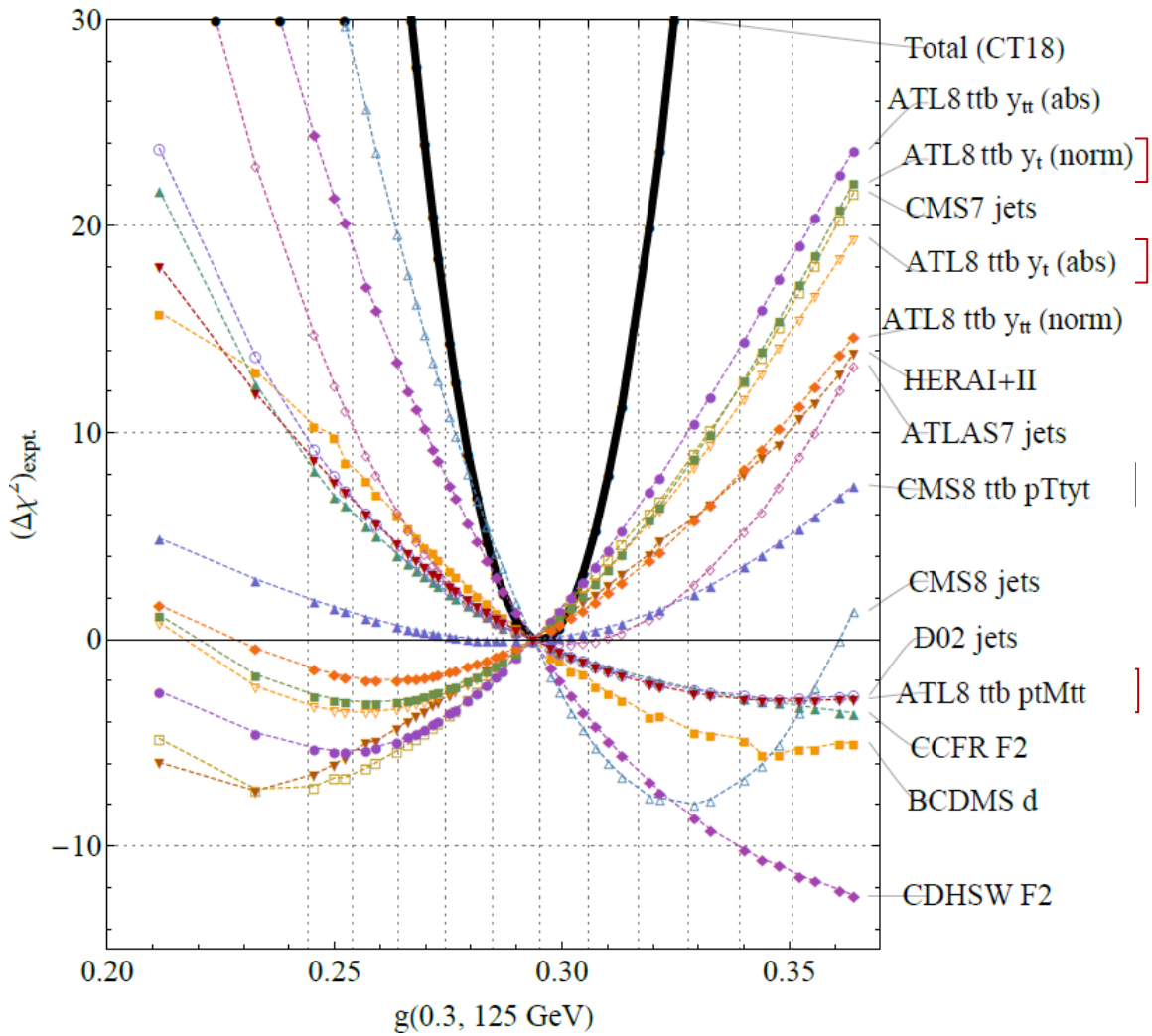
Projections with $\Delta\chi^2 = 1$ tolerance predict strong constraints on the gluon and other flavors.

Such projections effectively emphasize a given measurement over the other experiments.

Figure: An estimated reduction of the relative uncertainty on the gluon PDF by profiling CT14 PDFs using simulated $t\bar{t}$ measurements at the HL-LHC [CMS-PAS-FTR-18-015].

How constraining are $t\bar{t}$ data?

CT18 NNLO + unfitted ATLAS 8 TeV top single-diff. data



More realistic estimates account for multiple PDF functional forms and some disagreements between the measurements.

They predict milder impact from $t\bar{t}$ data

In the figure, pulls on the gluon from ATLAS8 $y_{t\bar{t}}$ and y_t distributions (absolute or normalized) agree with HERA DIS, oppose ATLAS8 $d^2\sigma/(dp_{T,t}dm_{t\bar{t}})$ and CMS8 $d^2\sigma/(dp_{T,t}dy_{t,ave})$

Impact of LHC 13 TeV $t\bar{t}$ production beyond CT18

[JHEP 01 \(2021\) 033, 2021 - arXiv: 2006.09274](#)

- ATLAS: Measurements of $t\bar{t}$ differential cross-sections at 13 TeV in the all-hadronic channel (1D); $36.1 \text{ fb}^{-1}\text{IL}$

[JHEP 1902 \(2019\) 149, 2019 - arXiv:1811.06625](#)

- CMS: Measurements of $t\bar{t}$ differential cross sections at 13 TeV using events containing two leptons (1D); $35.9 \text{ fb}^{-1}\text{IL}$

Label in data list	Npt	N. Corr sys unc	Exp	Corr Sys
5 20 ATL13mtt	9	67	ATLAS	Nuisance par: given
5 21 ATL13ytt	12	67	ATLAS	Nuisance par: given
5 22 ATL13HTtt	11	67	ATLAS	Nuisance par: given
5 23 ATL13pTt1	10	67	ATLAS	Nuisance par: given
5 24 ATL13pTt2	8	67	ATLAS	Nuisance par: given
5 25 CMS13mtt	7	6	CMS	Nuisan par: Sigma-K dec
5 26 CMS13pTt	6	5	CMS	Nuisan par: Sigma-K dec
5 27 CMS13yt	10	9	CMS	Nuisan par: Sigma-K dec
5 28 CMS13ytt	10	9	CMS	Nuisan par: Sigma-K dec

Working on including the 13 TeV lepton+jet channel from CMS (137fb^{-1})

These are all full phase space absolute measurements

Theory predictions: setup

- CMS: FastNNLO grids – [\(Czakon et al. 1704.08551\)](#)
- ATLAS: bin-by-bin NNLO/NLO K-factors generated by MATRIX [\(Catani, Grazzini, et al. PRD2019\)](#) (MATRIX: See M. Grazzini's talk on Wed)

The NLO QCD calculation is obtained using our in-house APPLGrid fast tables [\(Carli et al. EPJC 2010\)](#) for the public MCFM calculation [\(Campbell, Ellis JPG 2015\)](#)

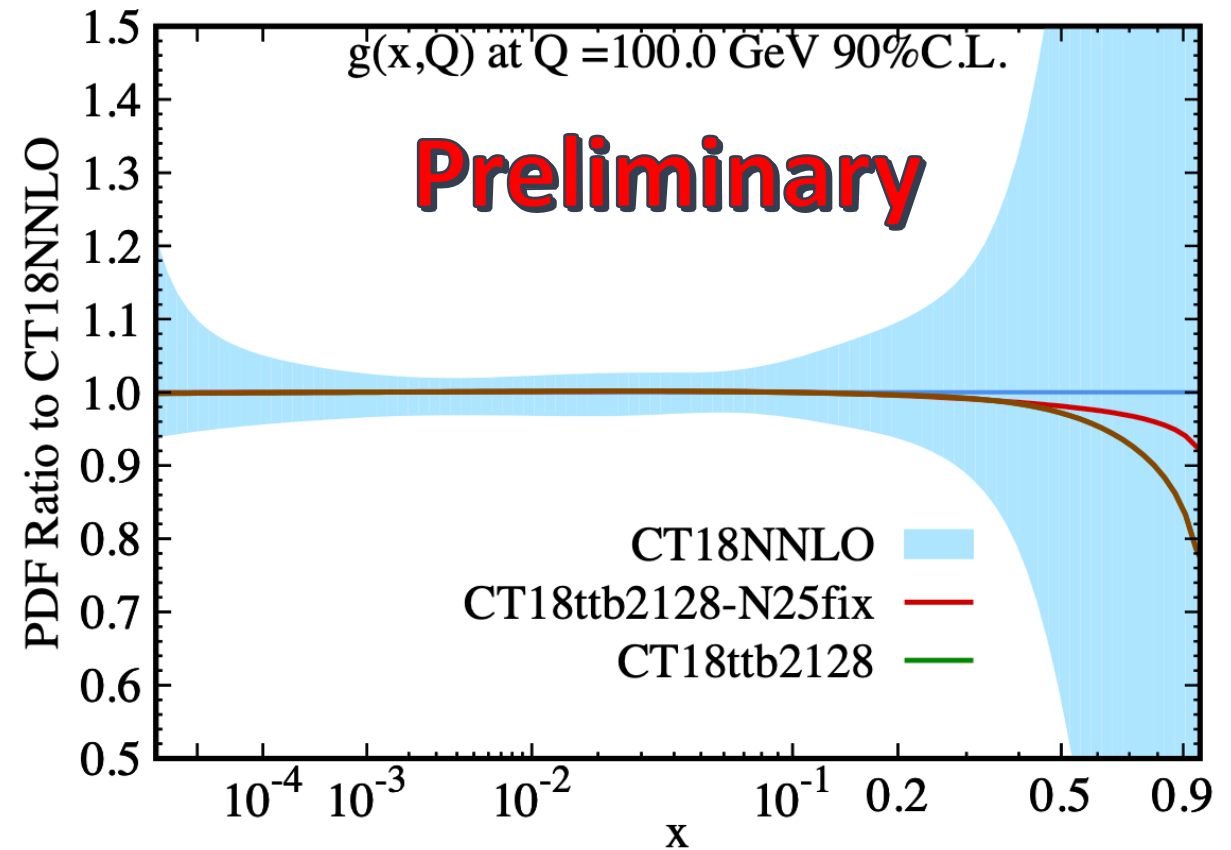
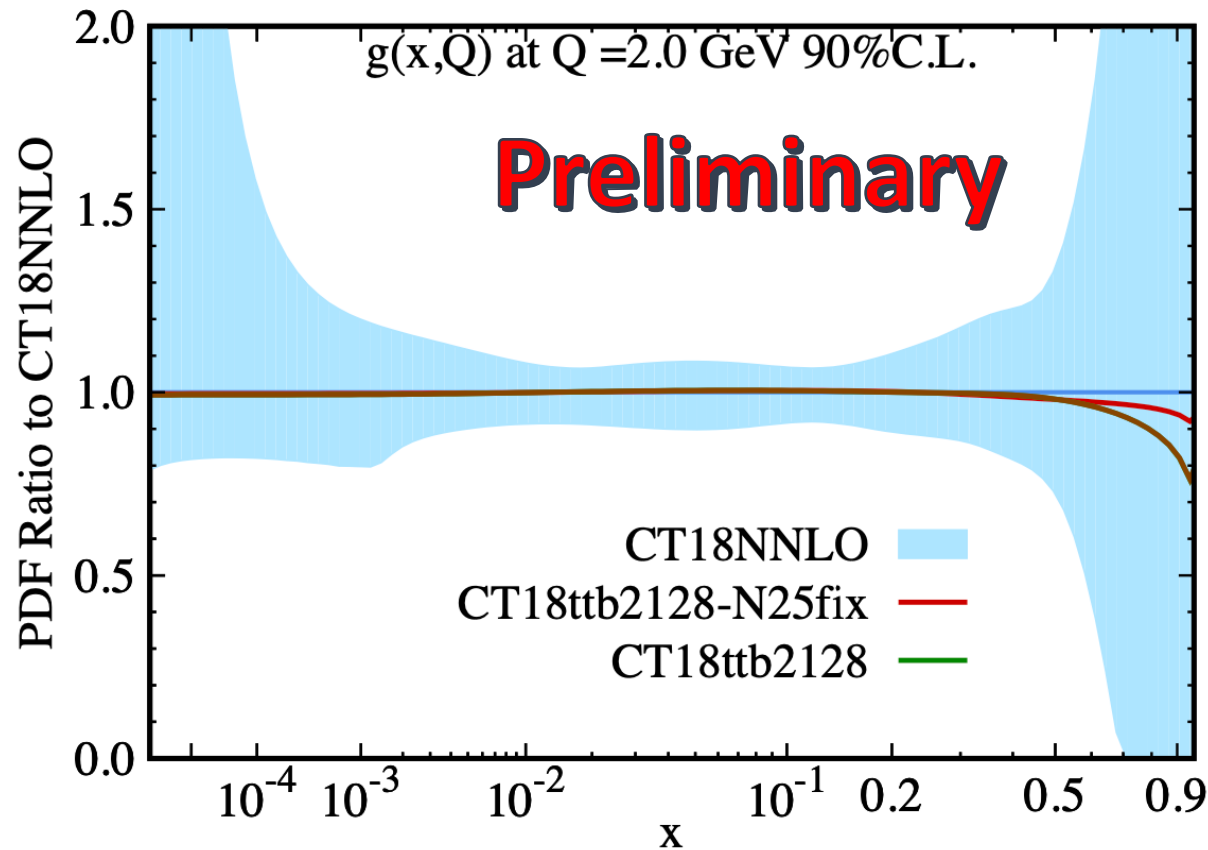
- $m_t(\text{pole}) = 172.5 \text{ GeV}$
- Fact/Ren scale choice:

$m_{tt}, p_{T,tt}, y_{tt}, y_t$ use $H_T/4$; $p_{T,t}$, use M_T ; $p_{T,t \text{ avg}}$ use $M_T/2$ [\(Czakon et al. JHEP 2017\)](#)

$$\mu_F = \mu_R = H_T/4 = \left(\sqrt{m_t^2 + p_{T,t}^2} + \sqrt{m_t^2 + p_{T,\bar{t}}^2} \right) / 4 \quad \mu_{F,R} = M_T^t/2 = \sqrt{m_t^2 + p_T^2}/2$$

- **EW corrections considered**: negligible impact on our fits.

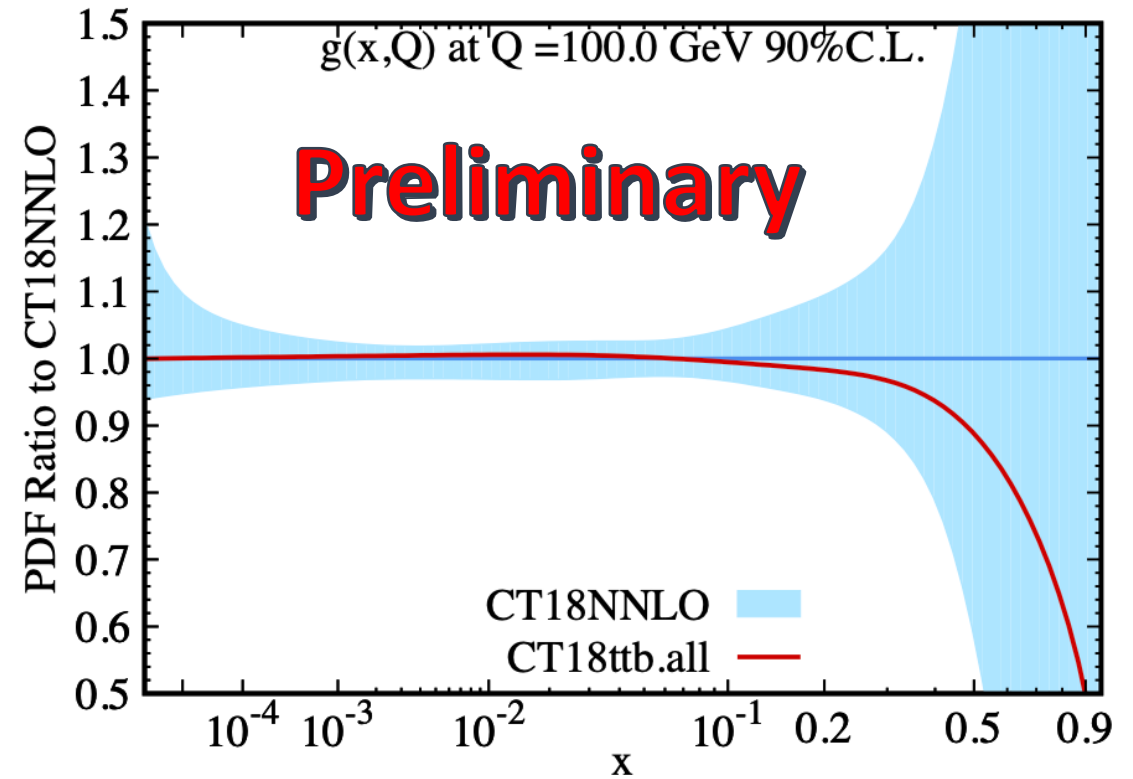
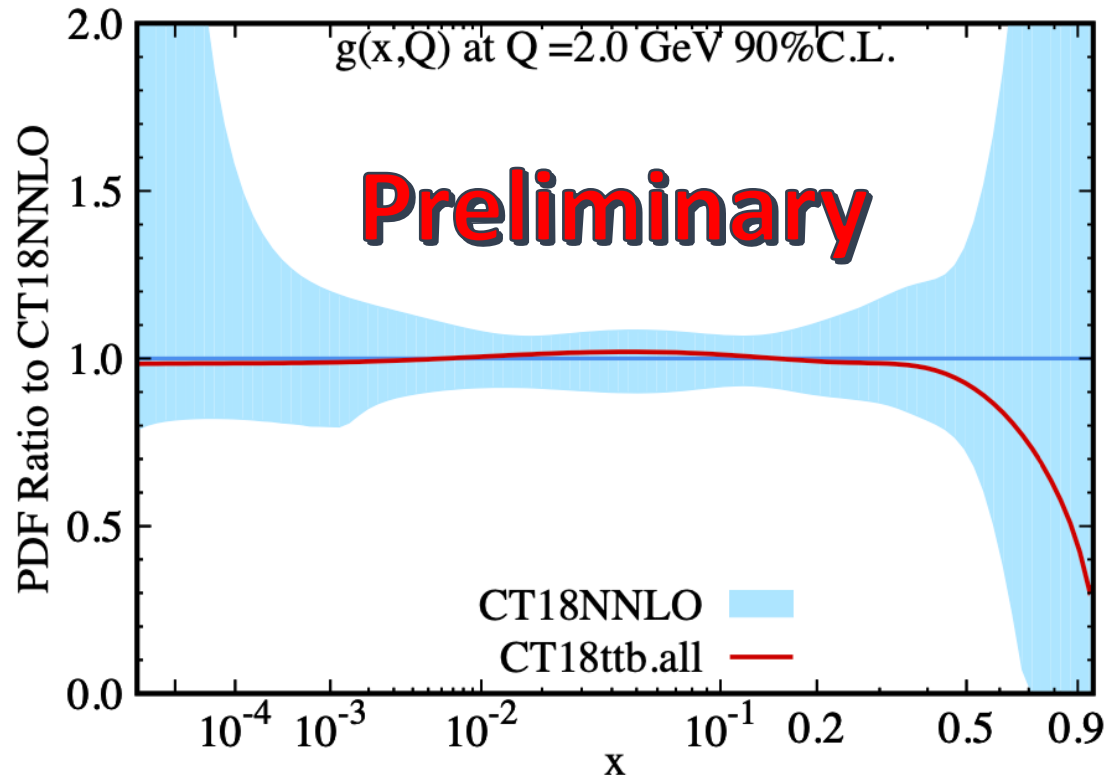
Global fit: Impact from y_{tt} 1D from CMS + ATLAS



ATLAS: DATA SET 521 ; NORM Fac = 1.00000 ; # of pts = 12 ; χ^2 = 12.796140 S= 0.29377 χ^2/N = 1.06634
 CMS : DATA SET 528 ; NORM Fac = 1.00000 ; # of pts = 10 ; χ^2 = 6.415790 S= -0.77071 χ^2/N = 0.64158

Pulls are in the same direction

Global fit: Impact from all $t\bar{t}$ data at 13 TeV ATLAS+CMS



ATL mtt DATA SET 520 ; $\chi^2/N = 1.42643$
 ATL ytt DATA SET 521 ; $\chi^2/N = 1.05387$
 ATL HTtt DATA SET 522 ; $\chi^2/N = 1.67374$
 ATL pTt1 DATA SET 523 ; $\chi^2/N = 1.29656$
 ATL pTt2 DATA SET 524 ; $\chi^2/N = 1.55261$
 CMS mtt DATA SET 525 ; $\chi^2/N = 2.96862$
 CMS pTt DATA SET 526 ; $\chi^2/N = 2.83397$
 CMS yt DATA SET 527 ; $\chi^2/N = 0.62119$
 CMS ytt DATA SET 528 ; $\chi^2/N = 0.52401$

Cumulative impact: gluon affected at $x > 0.1$
 Small impact at intermediate x

Stat. correlations between data ignored: **For illustrative purpose only**

Impact from new combined c- and b-quark production at HERA

(H1 and ZEUS Coll. 1804.01019)

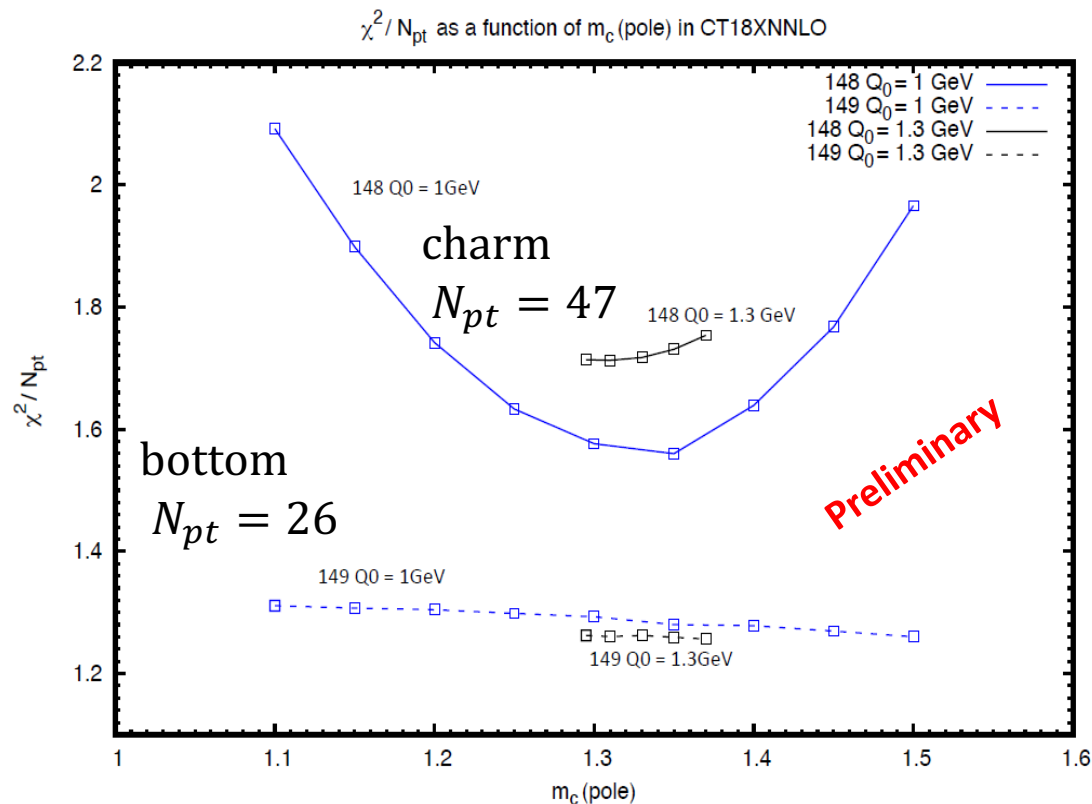


We fit these data using the SACOT- χ heavy-quark scheme at NNLO.

In all tried scenarios, we get χ^2/N_{pt} no less than 1.5, reached when the combined HERA HQ SIDIS data is included (even with large statistical weight)

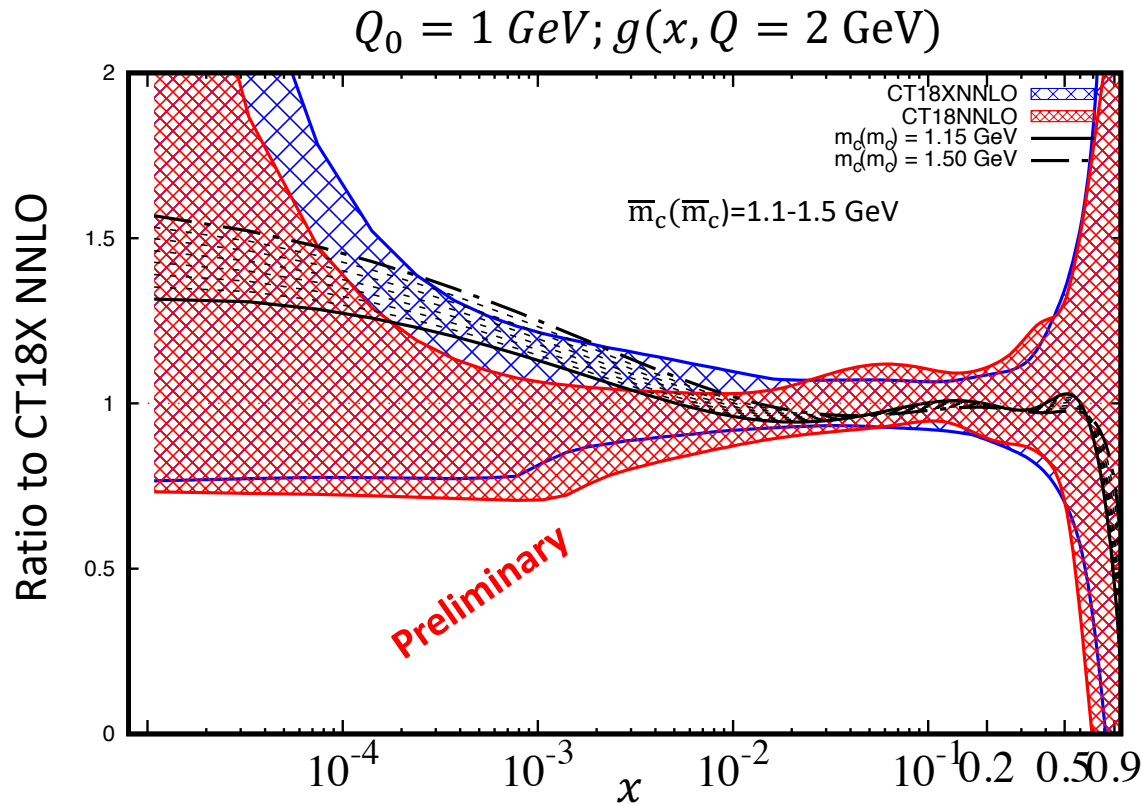
These data prefer a harder gluon at intermediate and small x .

Our χ^2 values are similar to those found by MSHT20 and to predictions from other groups reported in Table 4 of the HERA publication.



CT18XNNLO + combined HERA c/b DIS data set

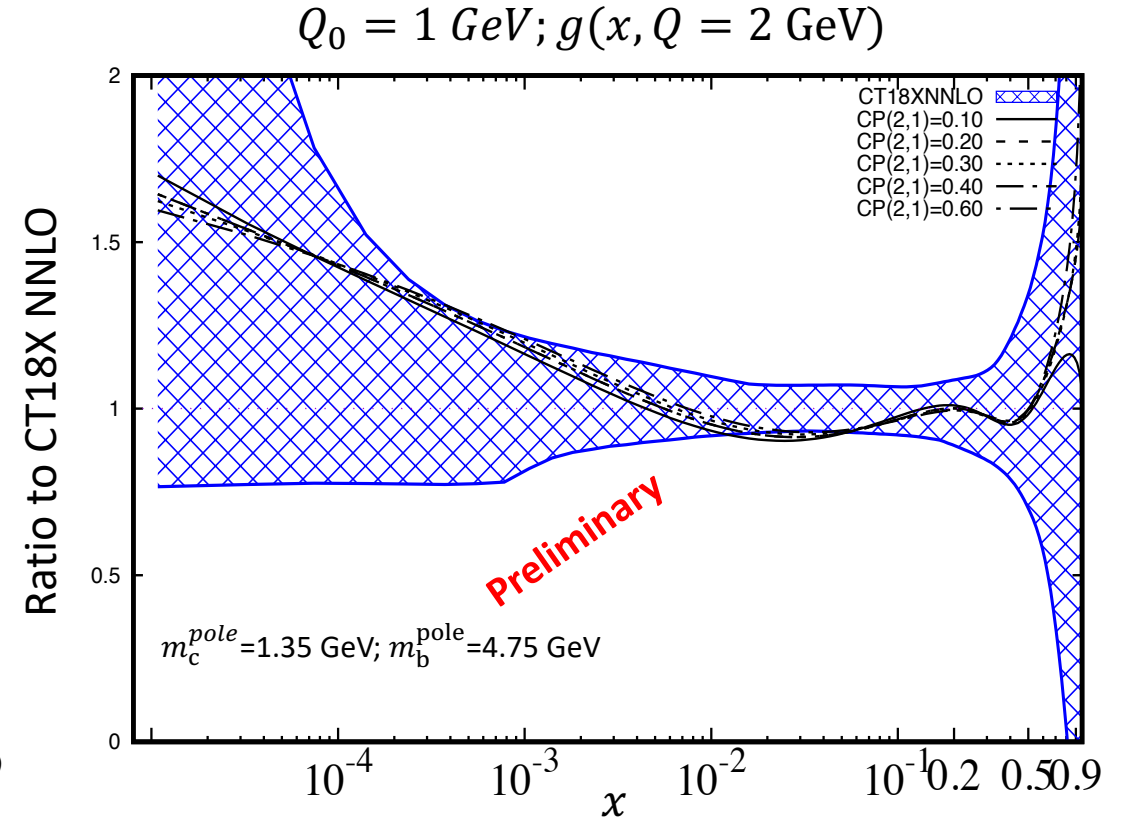
Fits with varied $\bar{m}_c(\bar{m}_c)$



This data set mildly prefers CT18XNNLO to CT18NNLO.

But χ^2/N_{pt} is never lower than 1.5 for all explored combinations

Fits with varied small-x scale



$$\mu_{DIS}(x) = A \sqrt{m_Q^2 + B^2/x^C}$$

Vary $B=CP(2,1)$, while keeping $A=0.5$ and $C=0.33$ fixed

Conclusions

- New GMVFNS applied to PP collisions: used to describe c/b production at central and forward rapidity
- Technically possible to generate predictions within the S-ACOT-MPS scheme at NNLO with suitable K-factors (NNLO/NLO) at hand.
- Easy to extend S-ACOT-MPS to other heavy-flavor processes,
- We explored the impact of 13 TeV $t\bar{t}$ LHC measurements on the CT18 PDFs
- Overall, the impact is found to be mild. This may change when $t\bar{t}$ prod. in lepton+jet ch @13 TeV is included.
- Impact of $t\bar{t}$ production at the LHC 13 TeV will further complement that of jet data on the gluon PDF, particularly in the large- x region.
- $t\bar{t}$ and jets overlap in the Q - x plane, but matrix elements and phase space suppression are different and constraints on the gluon PDF may be placed at different values of x .
- New c/b combination @HERA: deserves more attention. Important for small- x dynamics
- In general, HFs: critical to constrain m_Q , α_s , g -PDF correlations

BACK UP

Theory calculation & HF production dynamics

- In DIS, perturbative convergence of QCD calculations in the ACOT and other GM-VFN schemes at small momenta comparable to m_Q can significantly be improved by physical treatment of kinematics in flavor-excitation and subtraction terms.
- This is the motivation behind the S-ACOT-MPS (S-ACOT with massive phase space) factorization framework for heavy-quark scattering processes in proton-proton collisions.
- S-ACOT-MPS is equivalent to S-ACOT- χ but applied to proton-proton collisions.
- As for S-ACOT- χ , S-ACOT-MPS evaluates integrals of the Flavor Excitation and Subtraction terms using massless hard-scattering matrix elements combined with the mass-dependent, rather than massless, phase space.

S-ACOT GMVFN schemes

The literature related to development of GMVFN schemes is too vast and will not be discussed here.

We use S-ACOT-MPS to describe D-meson measurements at LHCb at 7 and 13 TeV [\[arXiv:2108.03741\]](#)

Another version, named S-ACOT- m_T , was developed by Helenius & Pakkunen (*JHEP* 05 (2018)) to describe D-meson data at LHCb and ALICE. S-ACOT-MPS differs in the mass treatment in the phase space.

S-ACOT-MPS results here are shown at NLO in QCD.

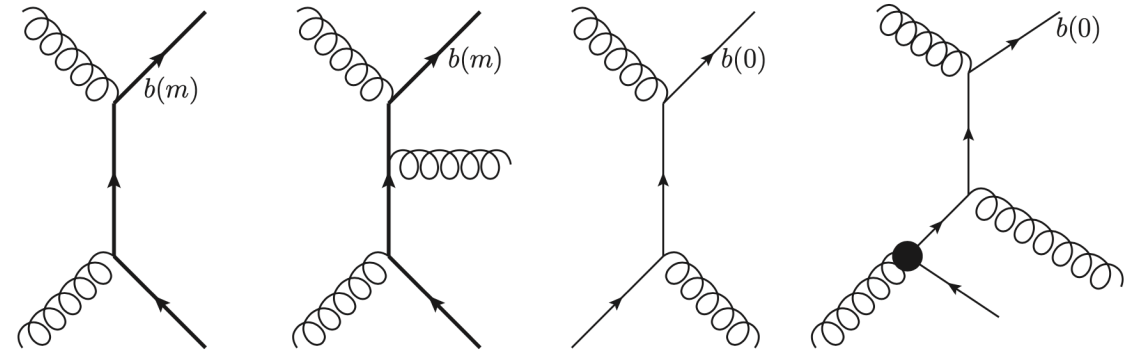
New NNLO predictions were recently made available:

- [FO calculation for Z + b-jet at \$O\(\alpha_s^3\)\$ in QCD, combines ZM NNLO and FFNS NLO.](#) Gauld, Gehrmann-De Ridder, Glover, Huss, Majer, 2005.03016
- [W + c-jet at NNLO at the LHC.](#) Czakon, Mitov, Pellen, Poncelet, 2011.01011

At this stage, it is already technically possible to generate predictions within the S-ACOT-MPS scheme at NNLO with suitable K-factors (NNLO/NLO) at hand.

Subtraction Heavy-flavor PDF

$$\tilde{b}(x, \mu) = \frac{\alpha_s(\mu)}{2\pi} \log \frac{\mu^2}{m_b^2} \int_x^1 \frac{d\xi}{\xi} P_{b \leftarrow g}\left(\frac{x}{\xi}\right) g(\xi, \mu).$$



Evaluated with DGLAP and stored in the \tilde{b} PDF. Then

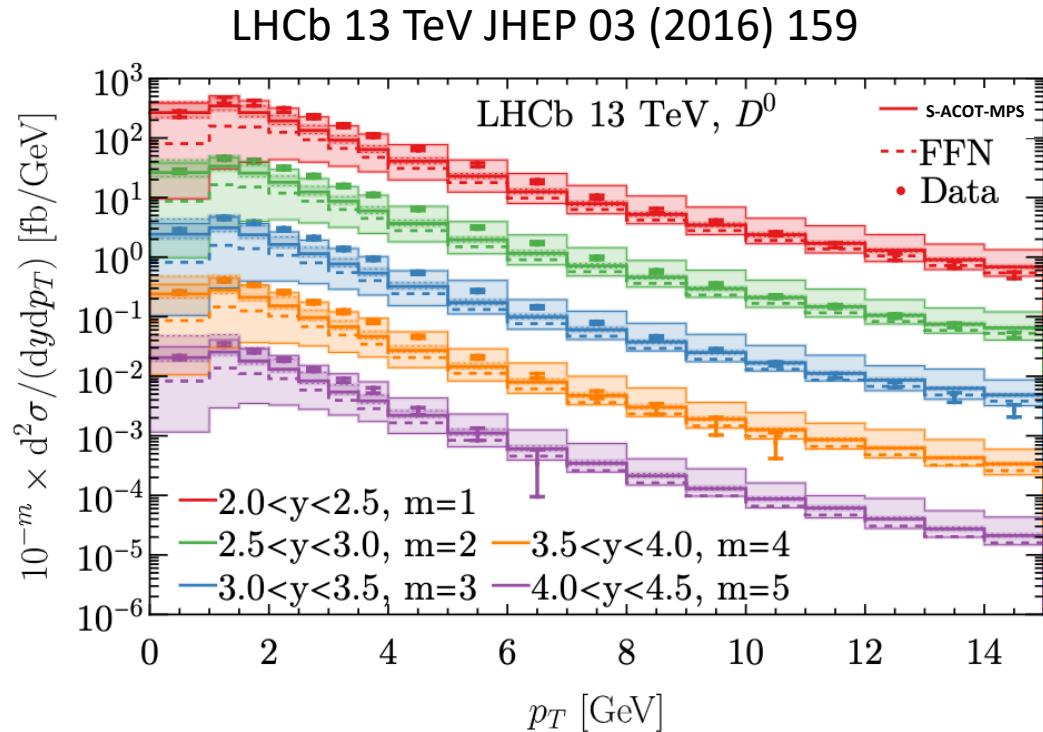
$$\sigma_{\text{FE}} = b(x_1, \mu) f_i(x_2, \mu) \otimes \hat{\sigma}_{bi}^{(0)} + (1 \leftrightarrow 2),$$

$$\sigma_{\text{SB}} = \tilde{b}(x_1, \mu) f_i(x_2, \mu) \otimes \hat{\sigma}_{bi}^{(0)} + (1 \leftrightarrow 2).$$

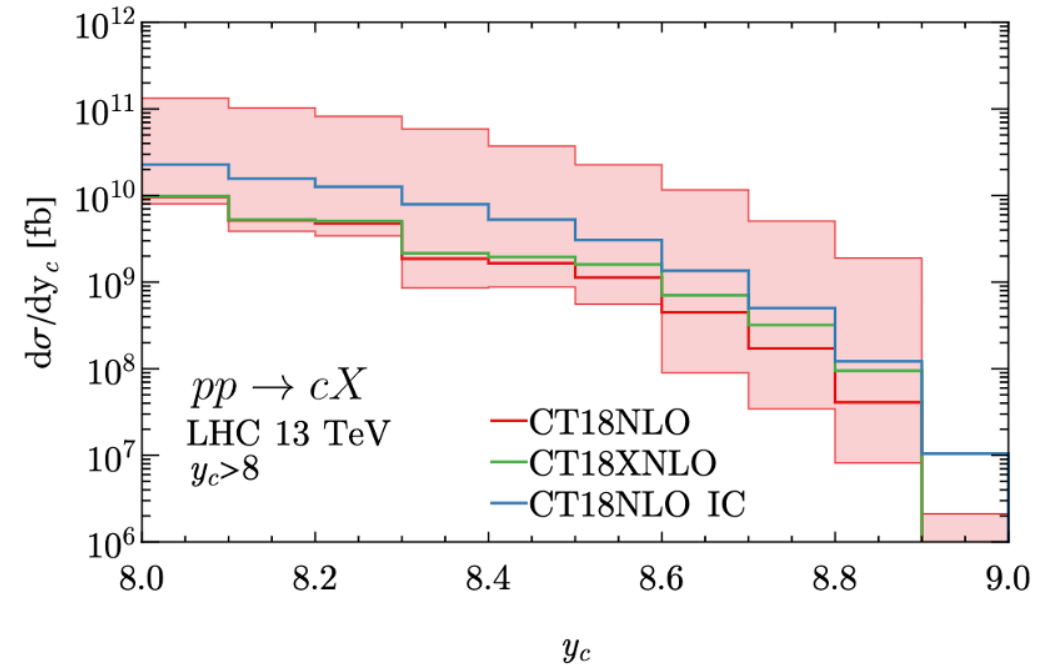
Can be done at the same time: the subtraction terms are calculated exactly as the Flavor Excitation terms, just by replacing the heavy flavor PDF by the subtraction PDF.

Using a subtraction/residual PDF, the subtraction terms are much faster to compute

Charm production at central and forward rapidity



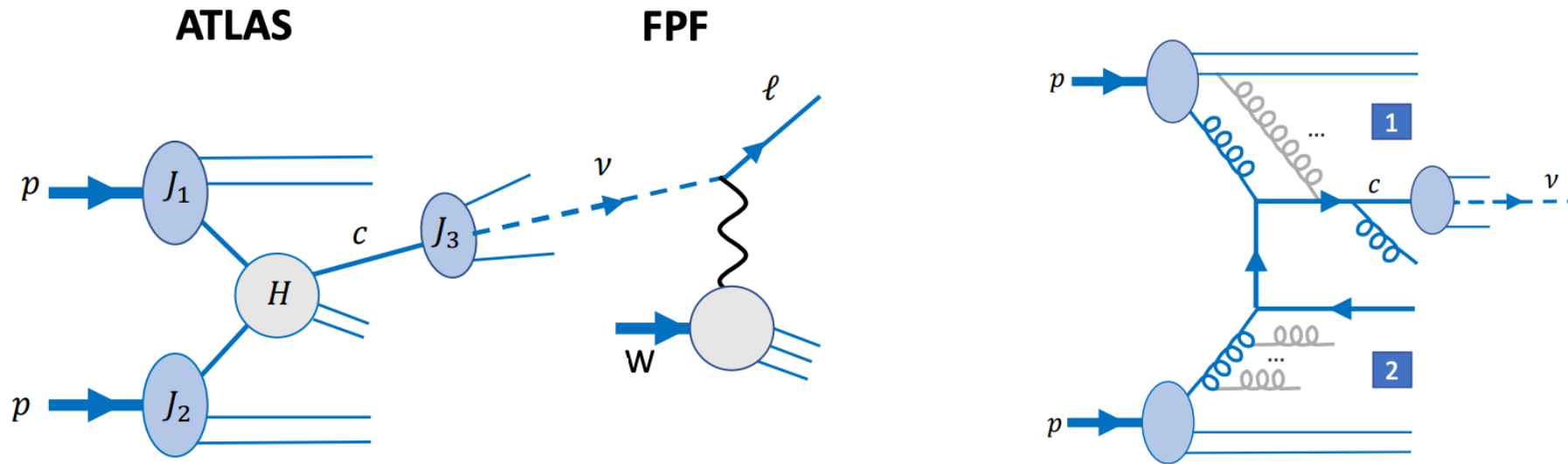
Transverse momentum at central rapidity at LHCb 13TeV.
Error bands are scale uncertainties.
[\[Xie, Campbell, Nadolsky, 2108.03741\]](#)



Prompt charm at the LHC 13 TeV in the very forward region ($y_c > 8$).
Error band represents the CT18NLO induced PDF uncertainty
at 68% C.L. [\[M.G., Xie, Nadolsky. FPF paper I, 2109.10905\]](#)

Probing IC content in the proton at FPF

Figure: Forward Physics Facilities I *Phys. Rep. 968 (2022)* 2109.10905



Forward neutrinos from charmed meson decays in ATLAS

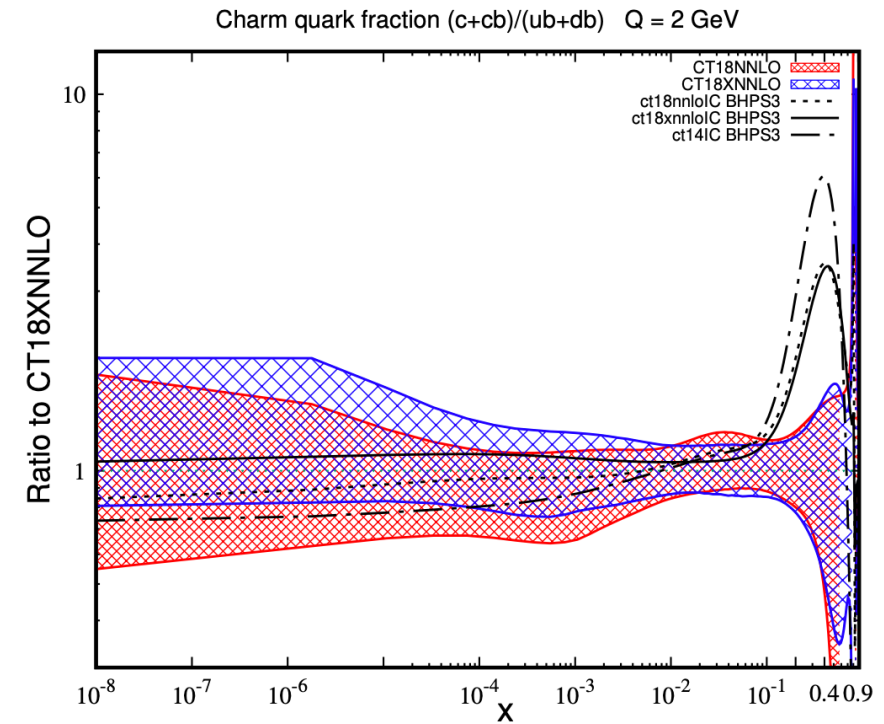
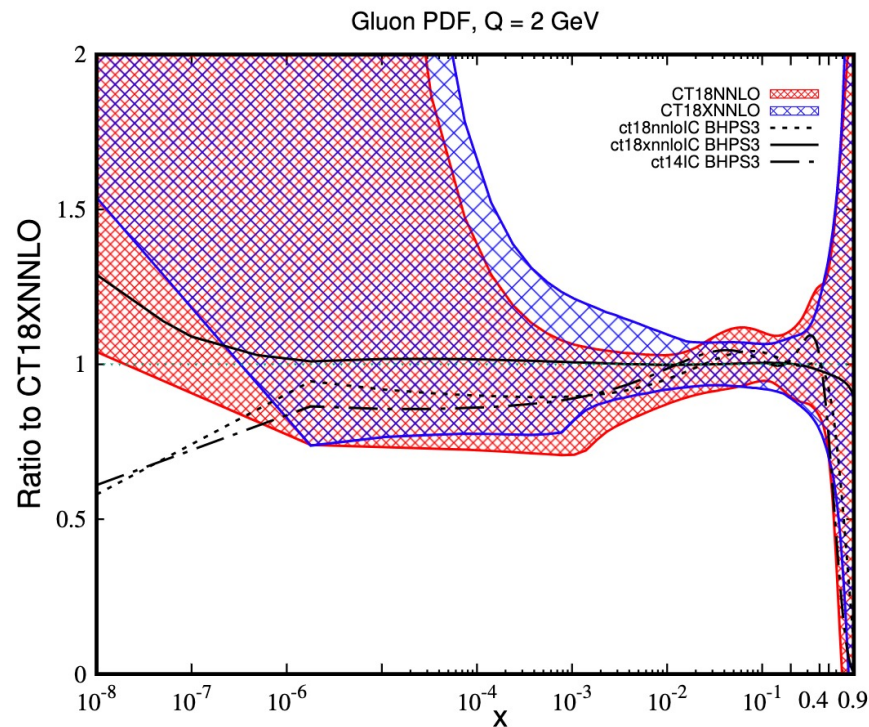
Production of a neutrino in the direction of the FPF. The charm quark escapes close to the beam axis in nearly the same direction as the comoving remnants of proton 1.

At large rapidity, one can probe QCD factorization beyond its standard formulation:

1. Enhanced power suppressed contributions: intrinsic charm
2. Large logarithms of the form $\ln(s/Q^2) \approx \ln(1/x)$: BFKL resummation framework

Probing IC content in the proton at FPF

NNLO gluon and charm-quark PDF in CT18/CT18X with IC. Error PDFs at 90% C.L. [[M.G. Xie, Nadolsky, FPF I paper 2109.10905](#)]



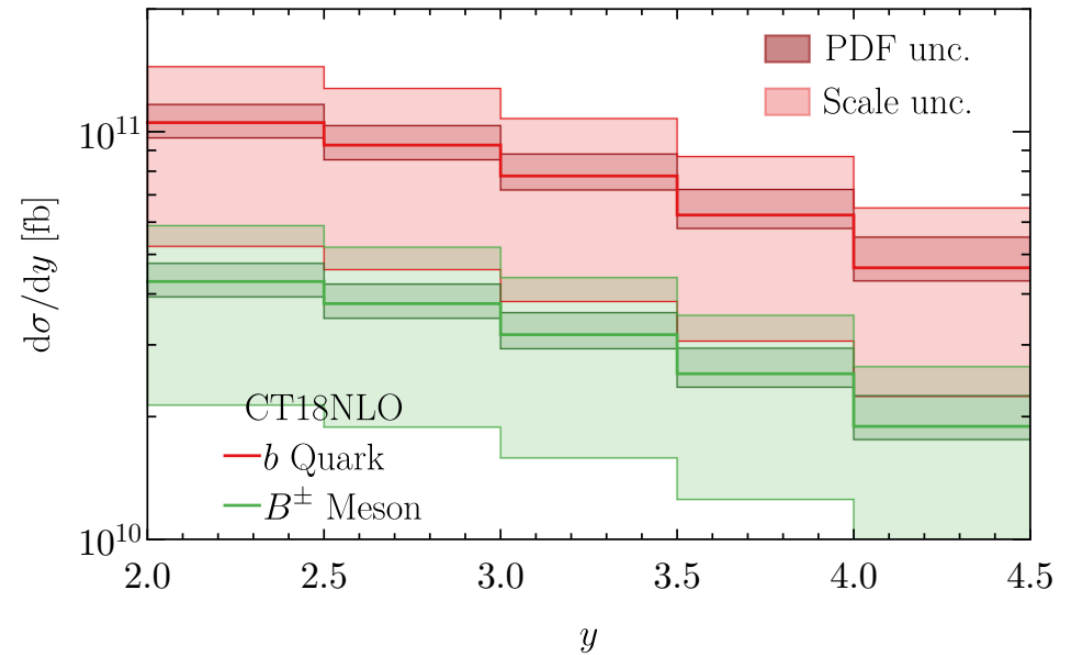
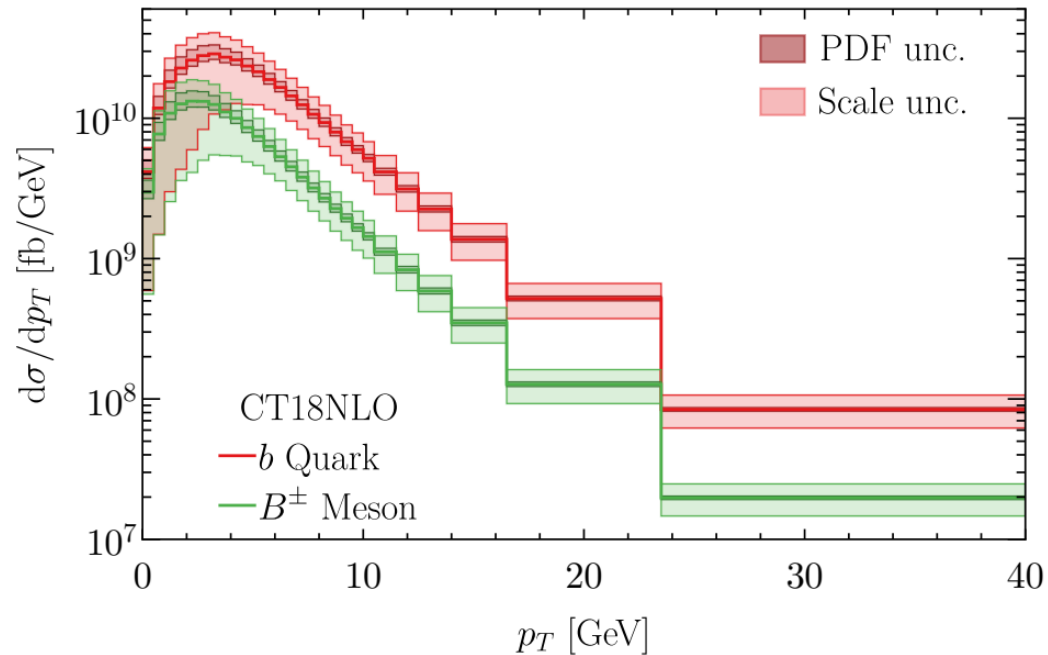
Charm hadroproduction and $Z + c$ production at the LHC can constrain the IC contributions.

In CT14IC, we looked at $Z+c$ at LHC 8 and 13 TeV. LHCb $Z+c$ data deserve attention as they can potentially discriminate gluon functional forms at $x \geq 0.2$ and improve gluon accuracy.

For small x below 10^{-4} , higher-order QCD terms with $\ln(1/x)$ dependence grow quickly at factorization scales of order 1 GeV.

FPF facilities like FASERv will access a novel kinematic regime where both large- x and small- x QCD effects contribute to charm hadroproduction rate.

Inclusive b-production: parton and particle level results



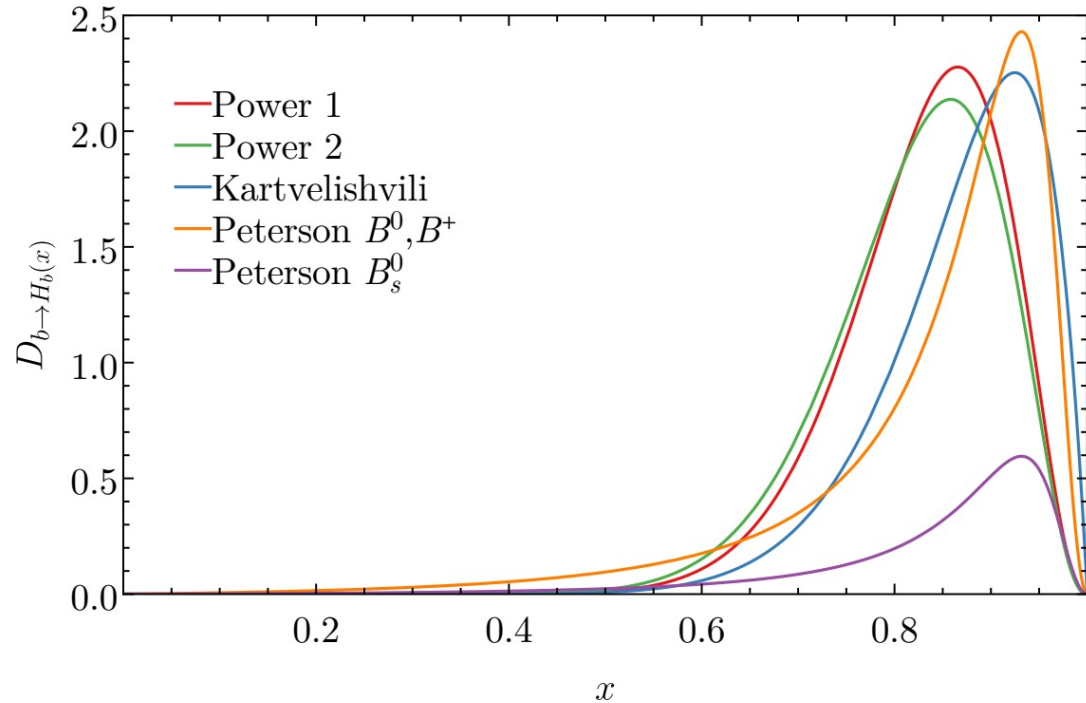
NLO theory predictions for the p_T and y distributions obtained with CT18NLO PDFs 90%CL at LHCb 13 TeV.

Parton-level distributions are plotted in red. Particle-level distributions are in green. [\[Xie, M.G., Nadolsky, 2203.06207\]](#)

Scale uncertainty is obtained from the 7-point variation by a factor of 2 using

$$\mu_R = \mu_F = \sqrt{m_b^2 + p_T^2}$$

A few details about b fragmentation

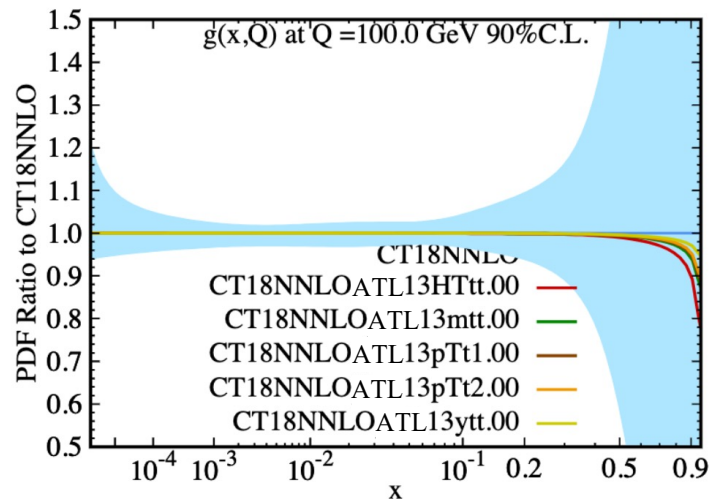
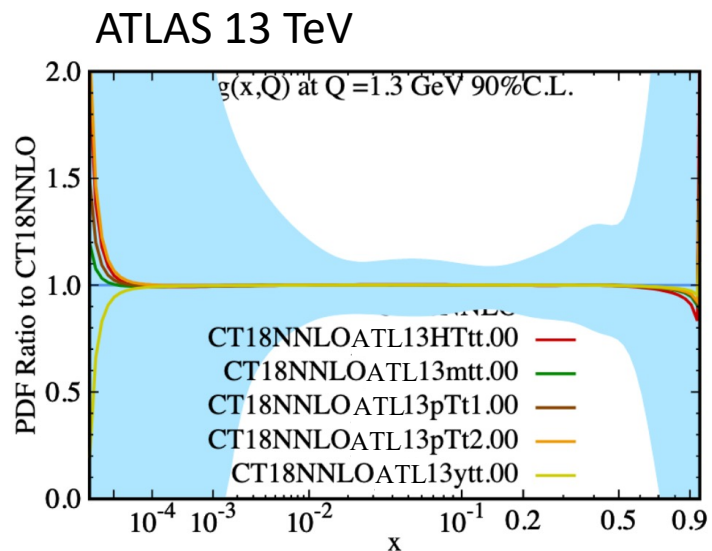


Left: Fragmentation functions for $b \rightarrow H_b$, modelled according to the power ansatz in Salajegheh et. al. [1904.08718], Kartvelishvili PLB (1978), and Peterson et. al. PRD (1983) parameterizations. The branch fraction is normalized to $\mathcal{B}(b \rightarrow B^0/B^+) = 0.408$

A conservative estimate of the uncertainty associated to the FFs in this work is obtained by considering relative differences between the parametrizations mentioned here. The corresponding branching fraction is normalized to $\mathcal{B}(b \rightarrow B_s^0) = 0.100$

A more rigorous estimate of FF uncertainties deserves a dedicated study which will be addressed in a future work.

ePump gluon PDF from ATLAS and CMS 13 TeV $t\bar{t}$ data

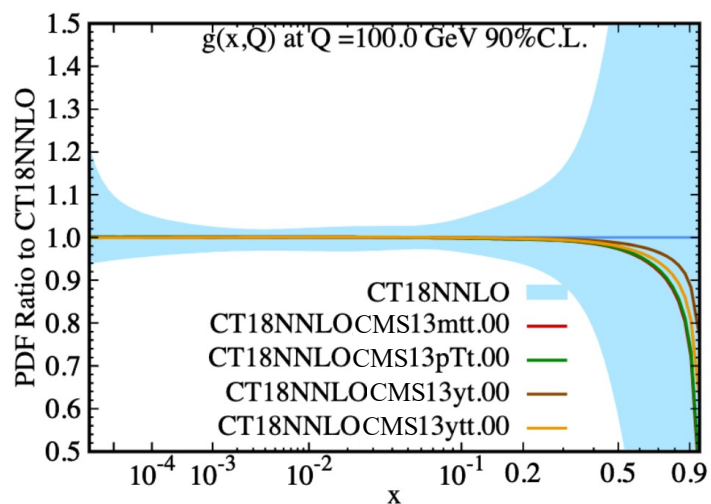
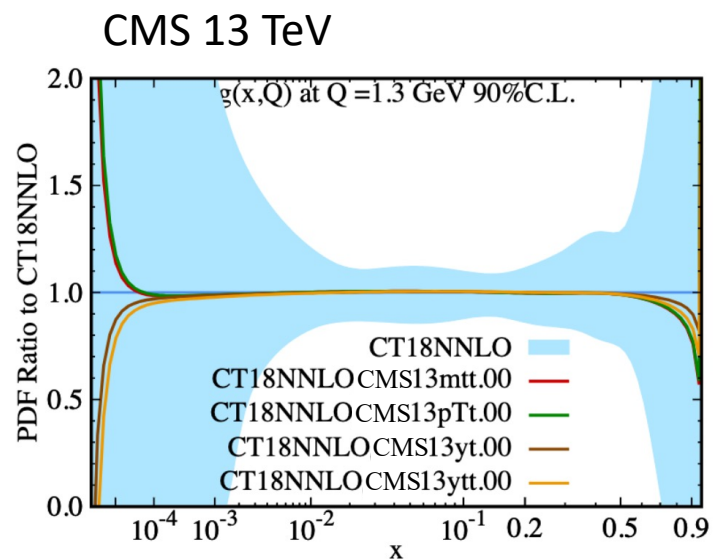


Here, data are included individually one at a time.

Error PDF Updating Method (ePump):
 impact from each individual data set from
 ATLAS and CMS at large x , ($x > 0.5$) at $Q=100$ GeV.

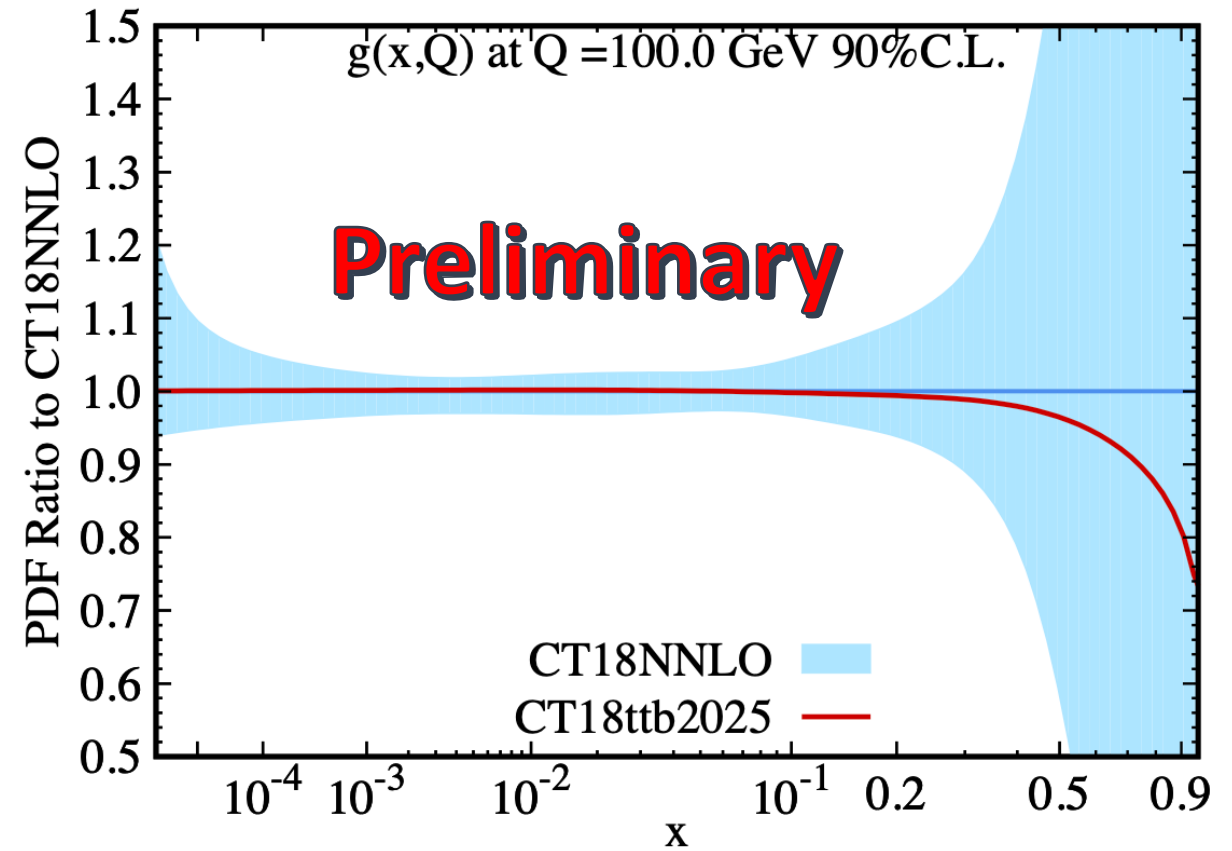
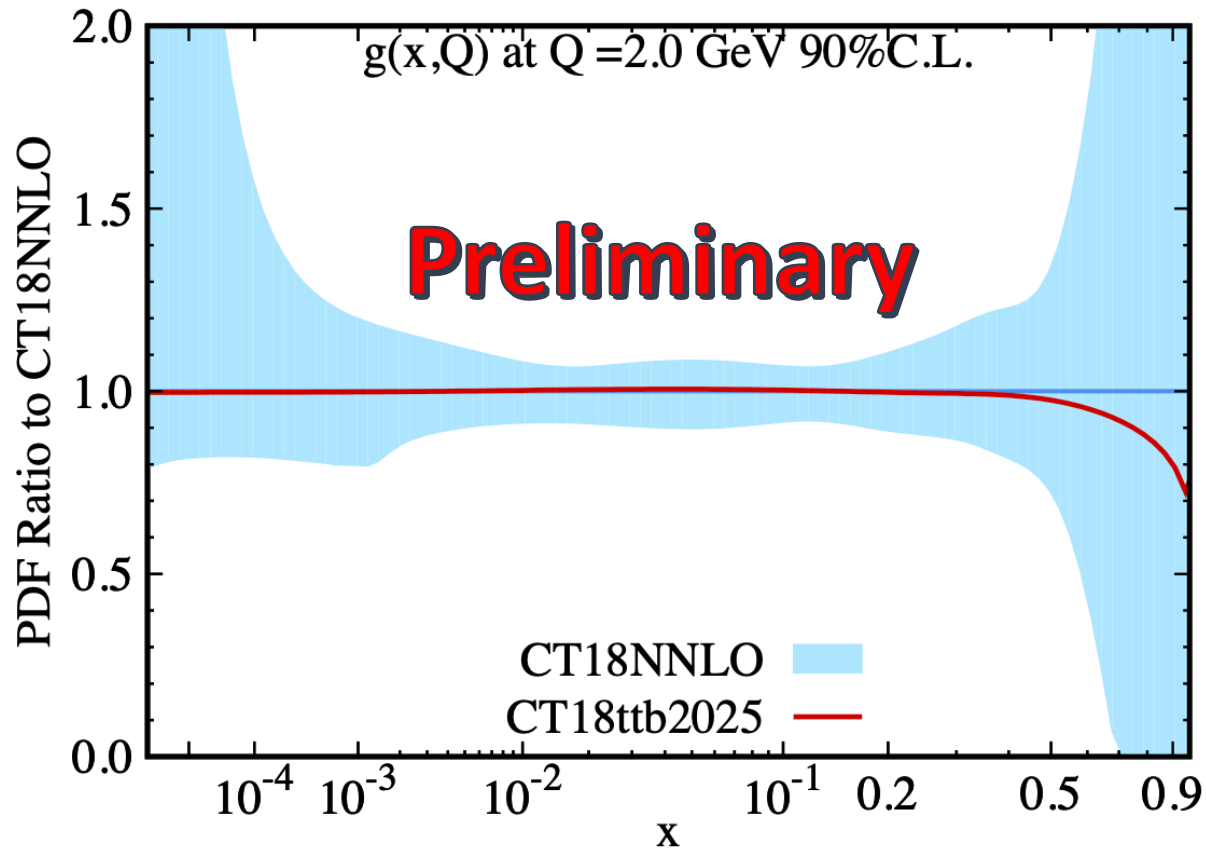
Pulls from different distributions at large x
 seem to be consistent.

ePump: Schmidt, Pumplin, and Yuan, PRD 2018



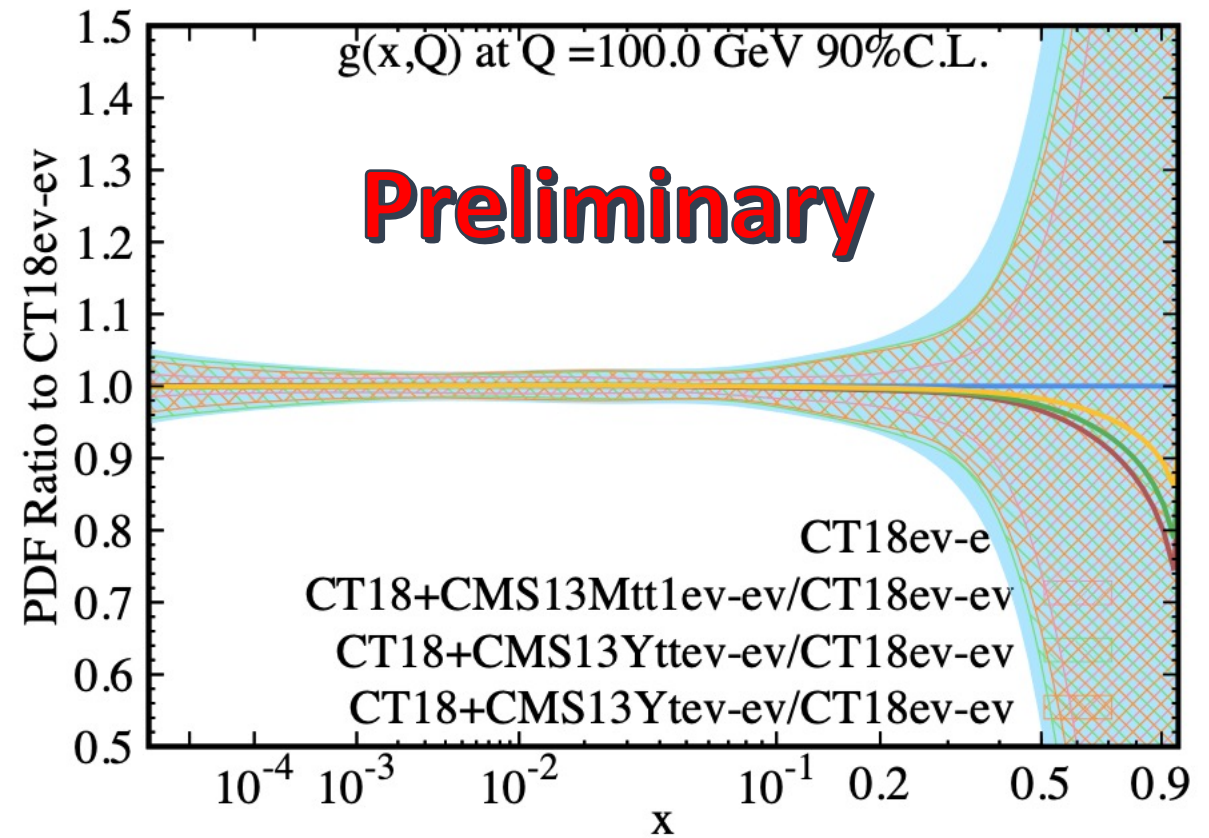
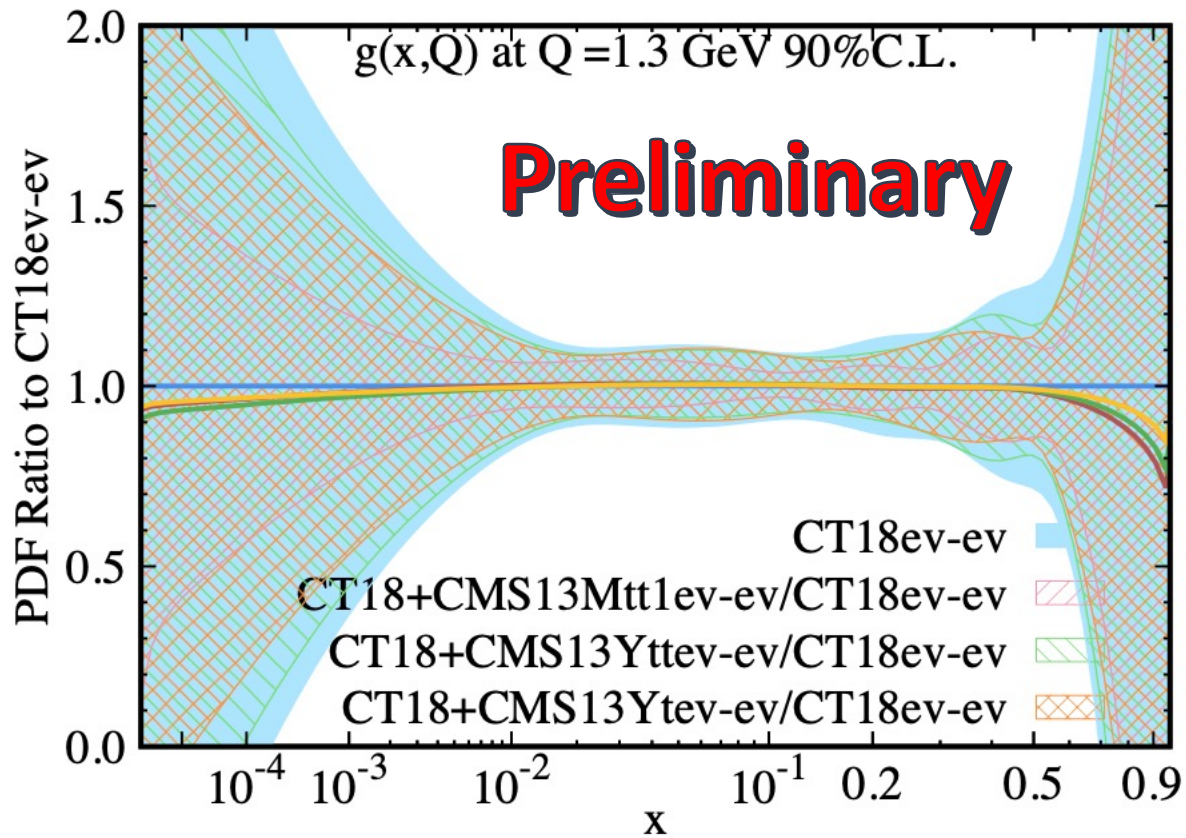
CT18NNLO 90% C.L.

Global fit: Impact from m_{tt} 1D from CMS + ATLAS



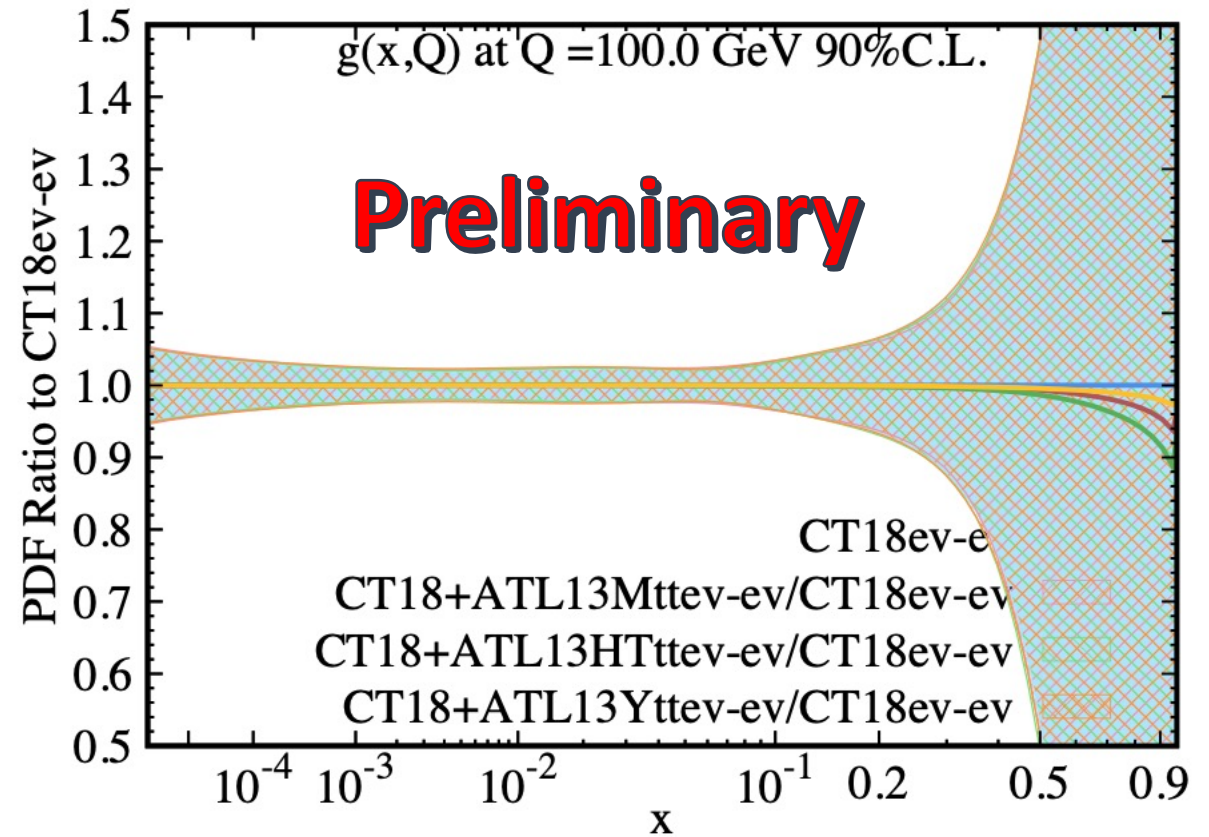
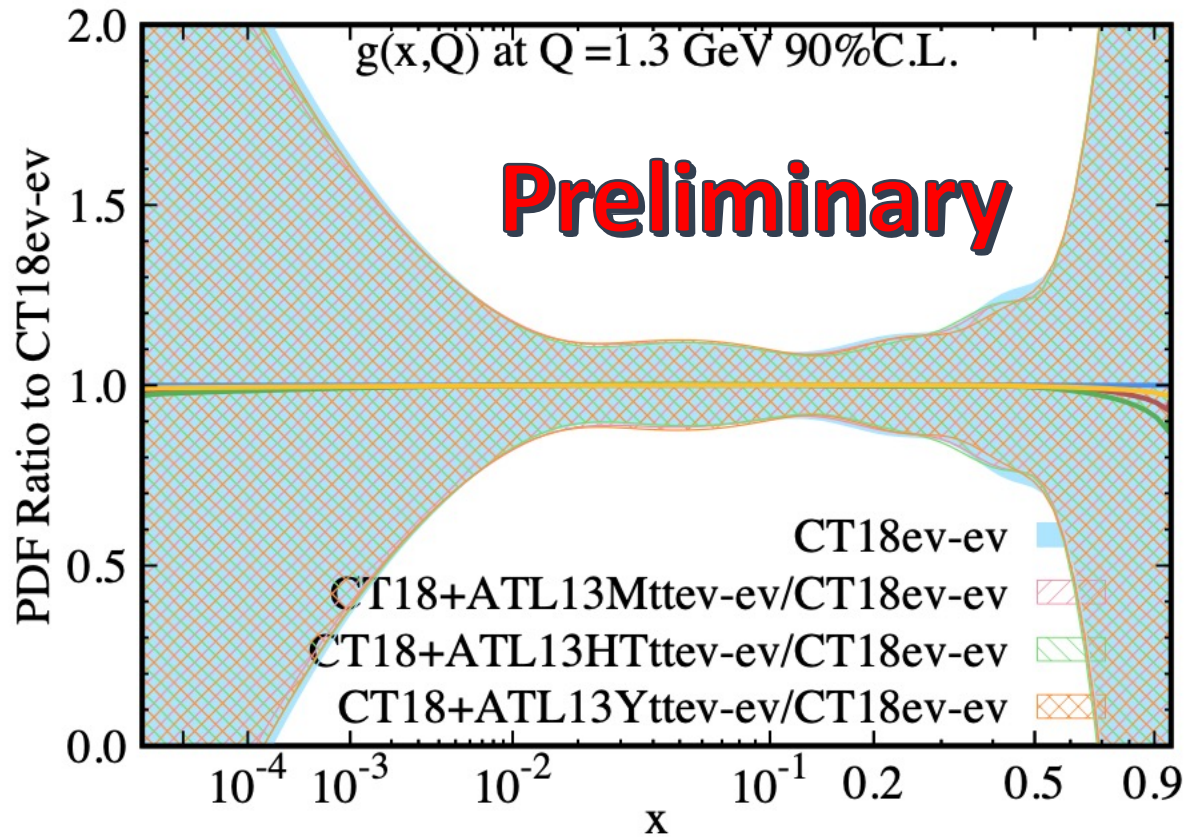
ATLAS: DATA SET 520 ; NORM Fac = 1.00000 ; # of pts = 9 ; χ^2 = 13.109893 S= 1.00223 χ^2/N = 1.45665
 CMS : DATA SET 525 ; NORM Fac = 1.00000 ; # of pts = 7 ; χ^2 = 22.179648 S= 2.82669 χ^2/N = 3.16852

Global fit: Impact from 1D distributions from CMS



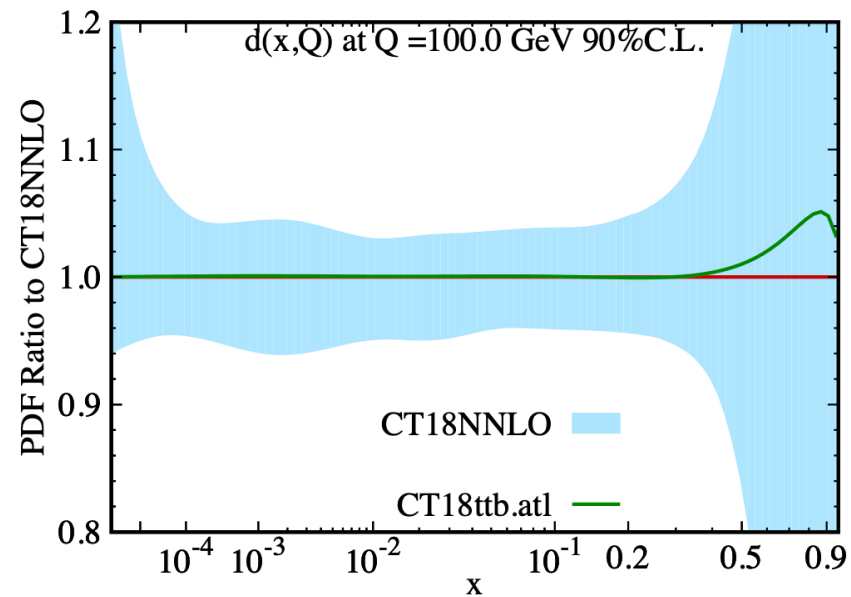
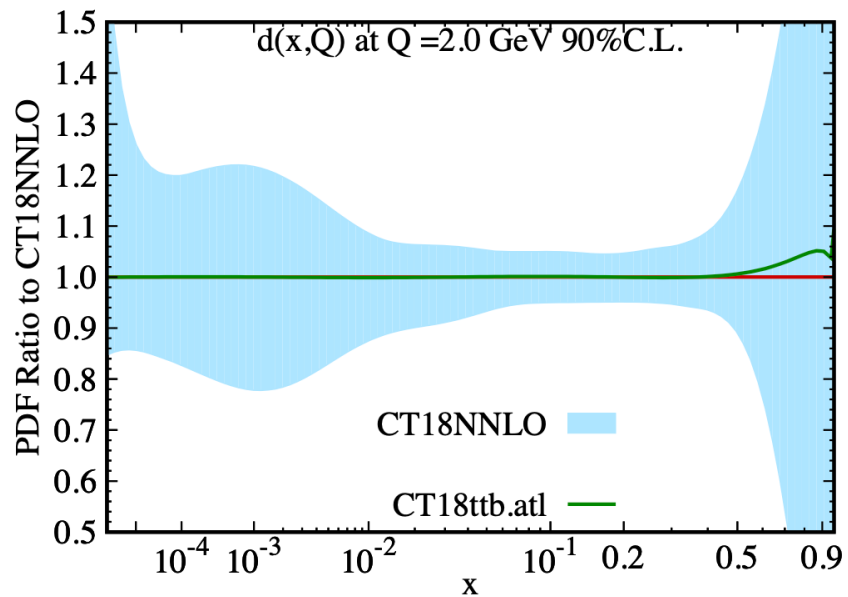
Data added one by one in the global analysis

Global fit: Impact from 1D distributions from ATLAS



Data added one by one in the global analysis

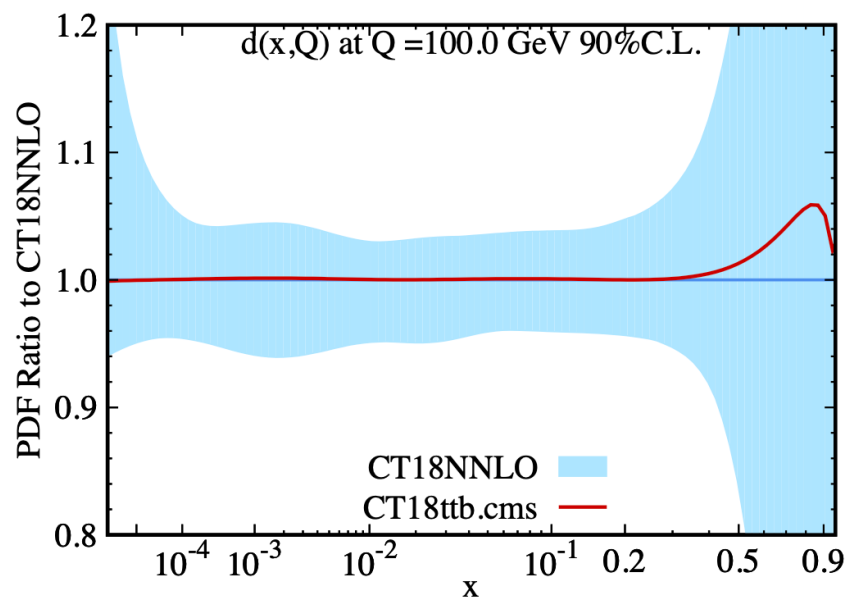
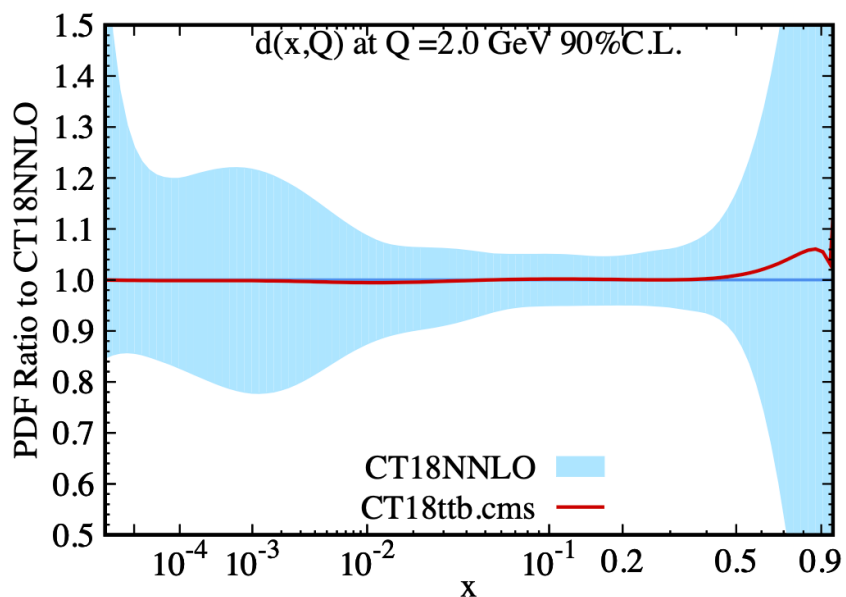
Impact from all ATL 1D: ytt, mtt pT1, pT2, Htt



For illustrative purpose only

There is a compensating effect on other PDFs, e.g., d and dv

Impact from all CMS 1D: yt, mtt pTt, ytt



For illustrative purpose only